Spring 2015

EFFECT OF IN VIVO POLYBROMINATED DIPHENYL ETHER (PBDE) TREATMENT ON HEPATIC GLYCERONEOGENESIS AND LIPID METABOLISM

Kylie Rose Cowens
University of New Hampshire, Durham

EFFECT OF *IN VIVO* POLYBROMINATED DIPHENYL ETHER (PBDE) TREATMENT ON HEPATIC GLYCERONEOGENESIS AND LIPID METABOLISM

BY

KYLIE R. COWENS
B.S. Biology, Norwich University, 2010
M.S. Kinesiology, University of Michigan, 2011

THESIS

Submitted to the University of New Hampshire
in Partial Fulfillment of
the Requirements for the Degree of

Master of Science
in
Nutritional Sciences

May, 2015

This thesis has been examined and approved in partial fulfillment of the requirements for the degree of Master of Science in Nutritional Sciences by:

Thesis Director, Gale B. Carey, Ph.D.
Professor, Department of Molecular, Cellular, and Biomedical Sciences

Joanne Curran-Celentano, Ph.D
Professor, Department of Molecular, Cellular, and Biomedical Sciences

Paul C. Tsang, Ph.D
Professor, Department of Molecular, Cellular, and Biomedical Sciences

On March 27, 2015

Original approval signatures are on file with the University of New Hampshire Graduate School.

ACKNOWLEDGEMENTS

I am very grateful for all who have supported me during this endeavor. Above all I would like to thank my family for their never-ending encouragement and pride in all that I do. They have given me the strength necessary to pursue any path I wish, and the courage to self-reflect and value happiness as my greatest success. They have played a large role in sculpting the person I am today, and words cannot express how much I value their support.

My committee members, Paul Tsang and Joanne Curran-Celentano, have provided additional, moral support through the ebbs and flows of my time at UNH, and I would like to thank them for their guidance. Tom Foxall was an invaluable member of the faculty as he provided a backboard against which I could discuss ideas and problems. Additionally, he offered his materials and machines for my use, which was key in helping me to finish lab work. I would also like to acknowledge my officemates Nicole Jaskiewicz and Angela Cicia, who were great friends and peers during this program.

Unarguably the most instrumental influence during my degree was my advisor, Gale Carey. She guided and challenged me as a scientist with great patience. She also helped me to harness my love of teaching, serving as an excited and well-practiced mentor in the classroom. I thank her for her belief in me and her support of my path, despite the twists and turns it may have taken.

TABLE OF CONTENTS

ABSTRACT

EFFECT OF *IN VIVO* POLYBROMINATED DIPHENYL ETHER (PBDE) TREATMENT ON HEPATIC GLYCERONEOGENESIS AND LIPID METABOLISM

by

Kylie R. Cowens

University of New Hampshire, May 2015

Polybrominated diphenyl ethers (PBDEs) are flame-retardant chemicals that contaminate the environment. Through ingestion and inhalation, these chemicals get into the human body, where they affect the liver by suppressing the metabolic enzyme phosphoenolpyruvate carboxykinase (PEPCK), which is partially responsible for glyceride-glycerol production via glyceroneogenesis. This study investigated the effects of PBDE-induced hepatic PEPCK suppression on glyceroneogenesis, and the associated perturbations in liver lipid metabolism. Twenty-eight male, weanling Wistar rats were treated daily with 14 mg/kg body weight PBDE mixture, DE-71 (TRT, n=14) or corn oil vehicle (CON, n=14) for 28 days. After a 48-hour fast, rats were sacrificed and blood and livers removed for analysis of serum metabolites, PEPCK protein levels, PEPCK activity, liver lipids, and glyceroneogenesis. TRT animals exhibited significant increases in serum ketones (27%), accompanied by significant decreases in serum triglycerides (27%), and liver PEPCK protein (23%), PEPCK Vmax (40%), lipids (29%), and glyceroneogenesis (41%) compared to CON. These findings demonstrate that

PBDE-induced PEPCK suppression impacts liver lipid metabolism, likely by suppressing glyceroneogenesis.

CHAPTER 1

LITERATURE REVIEW

POLYBROMINATED DIPHENYL ETHERS

Background

Polybrominated diphenyl ethers (PBDEs) are a class of brominated environmental chemicals that were incorporated into consumer products beginning in the 1970s to decrease flammability of home and office supplies such as electronics, furniture, and upholsteries (Watkins et al., 2011, Besis and Samara et al., 2012). Structurally, PBDEs are similar to thyroid hormone, with two phenyl rings connected by an ether bridge and the potential addition of 2-10 bromines in 209 possible combinations or congeners (see Figure 1).

Commercially, 3 main classes of PBDEs have been produced: deca-, penta-, and octa-BDE formulations. These nomenclatures refer to the degree of bromination within each class: deca-BDE compounds are a mixture of congeners that are nona- or deca-brominated; octa-BDE consist of mainly congeners that are hexa-, hepta, or octa-brominated; penta-BDE are made mostly from congeners that are tetra- or penta-brominated (McDonald, 2002).

The phasing out of commercially added penta- and octa- formulations began in the early 2000's, followed by the complete phase out of the deca- formulations by the end of 2013. There are currently no PBDEs in commercial use, but because PBDE-containing products exist in homes and offices (Costa et al., 2008), PBDEs continue to persist in the environment.

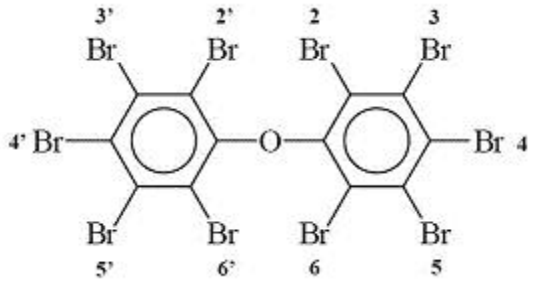

Figure 1 – Structure of PBDE: two phenyl rings connected by an ether bridge. Bromines can be added in any combination in the 10 positions indicated, with a minimum of 2 bromines and a maximum of 10. There are 209 possible combinations, or congeners.

PBDEs as environmental contaminants

PBDEs are not chemically bound to the products in which they are used, allowing for their easy transition into the environment by leaching into soil and groundwater upon disposal of PBDE-containing products in landfills. Furthermore, PBDEs contaminate the outdoor air during production and through incineration of disposed products (Osako et al., 2004, Hale et al., 2008). Once in groundwater, PBDEs are able to penetrate the food supply, affecting produce and more notably fish and game (Costa et al., 2008). Diet is

one route of exposure, although more recently indoor inhalation and ingestion of dust have been identified as significant contributors to human exposure (Costa et al., 2008).

Studies conducted over the past 10 years have indicated that in the US, PBDEs are present in sediment, sludge, and soil in addition to key dietary sources including marine animals, dairy products, and meat (Costa et al., 2008). Studies have found PBDEs to be relevant in the indoor environment as well, with significant levels settling in dust (Jones-Otazo et al., 2005, Wilford et al., 2005, Wu et al., 2007). PBDEs have been detected in tissues such as breast milk (Dunn et al., 2010), adipose tissue (Johnson-Restrepo et al., 2005), liver (Covaci et al., 2007), and serum (Sjodjin et al., 2004), with the greatest burden reported in adipose tissue and liver (Frederiksen et al., 2009). This illustrates a clear migration of PBDEs from the environment into the human body.

PBDEs in the body

PBDEs are highly lipophilic compounds, and as such, accumulate in adipose tissue (Johnson-Restrepo et al., 2005). Metabolism however, occurs most notably in the liver, which participates in oxidative hydroxylation and reductive debromination of parent PBDE compounds (Stapleton et al., 2009). Both hydroxylated and debrominated metabolites have been identified in human serum (Athanasiadou et al., 2008, Thuresson et al., 2006), although the distinct pathways responsible for PBDE degradation remain unclear (Stapleton et al., 2009). Studies have found hydroxylated metabolites to have similar in vivo effects as their parent PBDEs (Feo et al., 2013), or in some cases more

harmful effects (Canton et al., 2005), suggesting in vivo metabolism of PBDEs is a worthy concern.

Endocrine-disrupting effects

One well-studied consequence of in vivo PBDE exposure is perturbed thyroid hormone signaling. Due to the similarities in structure between PBDEs and thyroxine, an inactive form of thyroid hormone, studies have found that PBDEs competitively bind, and therefore antagonize thyroid receptors α and β (Meerts et al., 2000). Furthermore, PBDEs have an affinity for binding both transthyretin and thyroxine binding globulin, two transporters responsible for binding thyroid hormone in circulation (Marchesini et al., 2008, Hamers et al., 2006).

It has been shown in both rats and mice that triiodothyronine, the active circulating form of thyroid hormone, is affected by the presence of PBDEs. One study treated Sprague-Dawley rats daily for 30 days with 100, 300, or 600 mg/kg/day of BDE-209, the PBDE congener that is most abundant in human tissue samples (Lee et al., 2010). Results illustrated a significant decrease in serum triiodothyronine at all three doses used. This was accompanied by a decrease in serum TSH at 300 and 600 mg/kg/day (Lee et al., 2010). These results are supported by work conducted in a mouse model, in which male offspring of dams treated with 0, 10, 500, or 1500 mg/kg/day BDE-209 daily for 17 days illustrated a significant decrease in serum triiodothyronine at both 10 and 1500 mg/kg/day doses (Tseng et al., 2008).

Taken together, these data suggest exposure to PBDEs affects thyroid metabolism at several stages, including transport, binding, and hormone availability. Furthermore, thyroid hormone is a driver of metabolism, and disruption of transport and signaling of this key hormone raises concern of PBDE-induced metabolic perturbations.

Liver-specific effects

One organ that is a main target for chronic exposure of PBDEs is the liver (Costa and Giordana, 2007). Considering the role the liver plays in PBDE catabolism, most notably through oxidative hydroxylation (Stapleton et al., 2009), this organ is likely to suffer PBDE-associated consequences. The liver is in control of many crucial metabolic processes and perturbations in function could have both liver-specific, and systemic consequences.

Although there are limited studies to date focusing on enzymatic or metabolic consequences of PBDE exposure in the liver, several studies have illustrated hepatic-associated consequences that highlight the liver as an organ of concern. One key consequence of PBDE exposure is hepatic oxidative stress. Albina et al. (2010) treated adult male Sprague-Dawley rats with a single dose of 0, 0.6, or 1.2 mg/kg BDE-99, an environmentally relevant congener. Forty-five days after treatment, animals were euthanized and livers were analyzed for markers of oxidative stress. Key antioxidant enzymes including superoxide dismutase (SOD) and catalase (CAT) were found to be significantly upregulated in livers of treated animals, SOD at both treatment doses and CAT at the highest dose. Furthermore, the ratio of oxidized to reduced glutathione was

significantly increased, suggesting greater levels of reactive oxygen species associated with BDE-99 treatment compared to controls.

These data are further supported by work from An and colleagues (2011) in a study analyzing two PBDE metabolites, 6-hydroxylated and 6-methoxylated BDE-47, and their effects on a human hepatoma cell line, HepG2. An et al., found that DNA damage was caused by both of these metabolites in a dose-dependent manner, accompanied by an increase in SOD activity and a decrease in reduced glutathione. This suggests that both PBDEs and their metabolites increase hepatic oxidative stress.

Other hepatic perturbations include increases in overall liver weight and fat accumulation in response to PBDE exposure. Lee et al. (2010) found liver weight was significantly increased in rats treated with 600 mg/kg/day BDE-209 for 30 days compared to control animals. Furthermore, these animals exhibited fatty degeneration in histological analyses of the livers. This is supported by a study conducted by Bruchajzer et al. (2010) where administration of 200 mg/kg/day of PentaBDE for 14 days resulted in increased fatty deposition in the livers of female rats, accompanied by an increase in relative liver mass. Nash et al. (2013) also found an increase in overall liver weight and relative liver weight in male rats in response to 28 days of treatment with 14 mg/kg DE-71, a Penta-BDE mixture. This was accompanied by a significant increase in liver lipid percentage.

There has been little research on the effects of PBDEs on hepatic lipid or carbohydrate metabolism. In a recent study, Nash and colleagues (2013) found that after 28 days of daily treatment with 14 mg/kg DE-71, hepatic phosphoenolpyruvate

carboxykinase (PEPCK) activity was suppressed by 43%. PEPCK lies at the crossroads of hepatic carbohydrate and lipid metabolism, and disruptions in hepatic PEPCK activity could have significant metabolic consequences. Currently, metabolic consequences of PEPCK disruption by PBDEs are unknown.

PHOSPHOENOLPYRUVATE CARBOXYKINASE

Background

PEPCK is responsible for the decarboxylation and subsequent phosphorylation of oxaloacetate (OAA) to form phosphoenolpyruvate (PEP), using guanosine triphosphate (GTP) or inosine triphosphate (ITP) as an energy source, and yielding GDP or IDP, and CO_2 as byproducts (Hanson and Patel, 1994). The main product of the PEPCK reaction, PEP, is an intermediate metabolite of *gluconeogenesis*, and is essential for the *de novo* production of glucose in times of fasting (Hanson and Patel, 1994, Chakravarty et al., 2005, Yang et al., 2009). PEP is also an intermediate metabolite of *glyceroneogenesis*, and is necessary for the *de novo* formation of glycerol-3-phosphate, the backbone of triglyceride (Chakravarty et al., 2005, Yang et al., 2009). The production of glycerol-3-phosphate, via glyceroneogenesis, is necessary for hepatic reesterification of fatty acids during times of fasting, when systemic and hepatic fatty acid levels rise due to increased rates of lipolysis (Chakravarty et al., 2005). Thus, PEPCK is the first rate-limiting enzyme in both gluconeogenesis and glyceroneogenesis, responding to changes in diet and hormones, such as glucagon and glucocorticoids (Chakravarty et al., 2005, Yang et al., 2009). PEPCK is present in two

forms, a cytosolic (PEPCK-c), and a mitochondrial (PEPCK-m) form, and relative expression of the two forms is species-dependent. In humans, the relative expression is 50:50, PEPCK-c:PEPCK-m, while in rodents there is a much greater expression of PEPCK-c, accounting for approximately 90% of the total PEPCK (Hanson and Patel, 1994).

Metabolic roles

Gluconeogenesis

Gluconeogenesis allows for conversion of non-carbohydrate substrates to glucose by the liver in times of acute fasting, or by the kidney in times of long-term starvation (Hanson and Patel, 1994). Ablation of whole body PEPCK-c in mouse models caused significant reductions in blood glucose and the animals did not survive past 3 days of life, illustrating the importance of PEPCK-c's gluconeogenic function (Hakimi et al., 2005). Furthermore, whole body PEPCK-c deletion resulted in hepatic fat accumulation that was 2 to 3 times greater than controls, accompanied by elevated circulating ketones (Hakimi et al., 2005). These data suggest perturbed lipid metabolism as well.

Elimination of liver PEPCK-c in mouse models resulted in slight systemic hyperglycemia, in addition to reduced gluconeogenesis within the liver tissue (She et al., 2000, Hakimi et al., 2005). The resulting hyperglycemia is likely due to the ability of the

kidney to perform gluconeogenesis and thereby compensate for losses in liver gluconeogenic function.

These data illustrate that (1) liver-specific reductions in PEPCK-c reduce gluconeogenesis, (2) a reduction in hepatic PEPCK-c can be compensated for by renal PEPCK, and (3) a loss of whole body PEPCK-c perturbs hepatic triglyceride metabolism, as evidenced by fat accumulation in the liver and increased circulating ketones.

Glyceroneogenesis

The main role of glyceroneogenesis is the production of glycerol-3-phosphate, the activated form of glycerol used for esterification of fatty acids to form triglycerides (Chakravarty et al., 2005, Yang et al., 2009). This occurs largely in the liver, and to a smaller extent in the adipose tissue (Chakravarty et al., 2005, Yang et al., 2009). Studies focused on the origin of glycerol-3-phoshpate have demonstrated through deuterium-labeled water techniques that after an overnight fast, up to 65% of triglycerides synthesized in the liver and exported in VLDL contain a glycerol backbone produced via hepatic glyceroneogenesis (Kalhan et al., 2001, Kalhan et al., 2008), highlighting the importance of this pathway in regulating lipid homeostasis.

Reduced hepatic glyceroneogenesis, a proposed consequence of decreased hepatic PEPCK, should theoretically decrease available glycerol-3-phosphate, reducing the amount of fatty acid esterification in the liver and causing a build-up of hepatic fatty acids. This would enlarge the pool of available fatty acid substrate for ketone synthesis,

and subsequently increase circulating ketones, a known metabolic consequence of decreased PEPCK (Hakimi et al., 2005, Stark et al., 2014). In addition, it is expected that hepatic triglyceride formation would decrease and result in decreased serum triglycerides. Indeed, reduced serum triglycerides are associated with ablation of hepatic and renal PEPCK-m (Stark et al., 2014), but fat accumulation in the liver in response to a loss of PEPCK-c (Hakimi et al., 2005) is contrary to reduced glyceroneogenesis, and requires further investigation.

Unlike gluconeogenesis, a reduction in hepatic glyceroneogenesis cannot be compensated for by another tissue. Although there is significant PEPCK activity in white and brown adipose tissue, the lungs, the jejunum, and the acinar cells of the mammary gland, in addition to the liver and kidney (Hanson and Patel, 1994), none of these tissues compensate for losses in hepatic glyceroneogenesis. Adipose tissue has sufficient PEPCK to participate in glyceroneogenesis, however the enzyme is differentially regulated in this tissue. While hepatic PEPCK is upregulated in response to fasting conditions and rising glucagon, adipose tissue PEPCK is suppressed during fasting, allowing for an increase in fatty acid release. Instead, adipose tissue PEPCK is upregulated in response to insulin when fatty acids are being made in the liver, and thus fatty acids can be esterified and stored in adipose, adding another layer of control over circulating fatty acid levels (Chakravarty et al., 2005), which are linked to diabetes and cardiovascular disease. Because of this lack of compensation, a PBDE-induced decrease in hepatic PEPCK may have a greater effect on whole body triglyceride metabolism, compared to carbohydrate metabolism.

There is no available data on how PBDE or other environmental chemicals may affect liver glyceroneogenesis, although there is relevant data from adipose. Recent work found that decreased PEPCK-c protein in adipose tissue caused by leptin was accompanied by decreased rates of glyceroneogenesis (Jaubert et al., 2012), highlighting the link between PEPCK-c suppression and the physiological consequence of depressed glyceroneogenesis. Due to the high rates of glyceroneogenesis present in the liver compared to the adipose tissue, combined with the suppression of hepatic PEPCK by PBDE, disrupted glyceroneogenesis is a likely, but currently unsupported, metabolic consequence of PBDE exposure.

METABOLIC AND HEALTH CONSEQUENCES OF DEPRESSED GLYCERONEOGENESIS

Metabolic consequences

There are three possible serum markers of decreased hepatic glyceroneogenesis: elevated fatty acids, elevated ketones, and suppressed triglycerides. Because hepatic glyceroneogenesis is largely responsible for esterification of fatty acids synthesized *de novo* by the liver (Kalhan et al., 2001, Kalhan et al., 2008), a decrease in glycerol-3-phosphate could lead to elevated hepatic fatty acids, which could be released into the blood stream, or act as a substrate for ketone synthesis in the liver. Although glyceroneogenesis has not been evaluated specifically, studies evaluating the effects of decreased PEPCK-c and decreased PEPCK-m have demonstrated an increase in serum ketones, most notably beta-hydroxybutyrate (Hakimi

et al., 2005, Stark et al., 2014). Increases in fatty acids and ketones would theoretically be accompanied by suppressed hepatic triglyceride formation, subsequently decreasing hepatic triglyceride output. Studies have reported variable changes in serum triglycerides in response to losses in PEPCK-c vs. PEPCK-m function (Hakimi et al., 2005, Stark et al., 2014), and the role of glyceroneogenesis in relation to these changes has yet to be addressed.

Health consequences

Insulin Resistance

It has been fairly well established that increases in circulating fatty acid levels are associated with the development of insulin resistance (Boden, 1991, Boden, 1997, Boden, 2006). After infusing human subjects with triglycerides and heparin to increase plasma free fatty acids, Boden used a euglycemic-hyperinsulinemic clamp to demonstrate that increased fatty acids significantly decreased glucose uptake in the presence of excess insulin, suggesting the development of acute insulin resistance that was both dose-dependent and reversible (Boden, 1997). Further work using euglycemic-hyperinsulinemic clamps supported this development of insulin resistance by demonstrating that a 35% decrease in glucose infusion rate was required to sustain euglycemia in rats treated with lipid/heparin and excess insulin (Griffin et al., 1999). Griffin found evidence to suggest fatty acid disruptions in insulin signaling may be occurring, and reported that elevated fatty acids affect 3 key steps involved in insulin-stimulated glucose uptake in muscle: (1) membrane-association of protein kinase C Θ,

(2) insulin receptor substrate-1 tyrosine phosphorylation, and (3) PI3-kinase activity. These decreases were accompanied by a 25% reduction in glucose transport in vivo (1999). Current research is focused on further elucidation of the mechanisms involved in fatty acid-induced insulin resistance, expanding on the work done by Griffin and colleagues (Capurso and Capurso, 2012). An unanswered question is: what are the mechanisms by which circulating free fatty acids may be increasing, and are metabolic disruptions of glyceroneogenesis contributing to this increase?

Vascular Disease

Elevation of ketone bodies is implicated in the development of vascular disease, a complication that is often associated with type 1 and type 2 diabetes (Rains and Jain, 2014). Although current review of the literature suggests that a mild elevation in circulating beta-hydroxybutyrate (BHB) may be cardioprotective (Dedkova and Blatter, 2014), recent studies have found that more marked increases in circulating ketone bodies, including BHB and acetoacetate (AA) may contribute to increased oxidative stress in endothelial tissue, potentially contributing to vascular disease (Rains and Jain, 2014, Kanikarla-Marie and Jain, 2015). A recent study using primary human umbilical vein endothelial cells demonstrated that treatment with BHB and AA caused a significant increase in reactive oxygen species (ROS). The addition of glucose to the media increased ROS to a greater extent (Kanikarla-Marie and Jain, 2015), suggesting that the presence of elevated ketones in combination with elevated glucose may have the most detrimental effect. This suggests that hyperglycemia due to diabetes could

further compound the oxidative stress accompanied by increased circulating ketones. Taken together, these data imply that the potential consequences of suppressed glyceroneogenesis, including increased fatty acids and increased ketones, could cause perturbations that work in concert to disrupt insulin sensitivity and vascular health.

SUMMARY

PBDE are environmental chemicals that are present in the human body and have known effects on the liver. Chronic PBDE exposure has been shown to suppress hepatic PEPCK activity, a key enzyme involved in both carbohydrate and lipid metabolism in the liver. While the kidney can compensate for losses in PEPCK-driven glucose metabolism, there are no documented tissues or pathways that can compensate for losses in PEPCK-driven lipid metabolism, including glyceroneogenesis.

HYPOTHESIS

PBDE-induced suppression of PEPCK activity decreases hepatic glyceroneogenesis and perturbs lipid metabolism.

CHAPTER 2

METHODS

ANIMALS

Experimental model and basic design

The male Wistar rat model was used for all experiments. A total of 28 rats were received from Charles River Laboratory (Wilmington, MA) weighing 75 to 100 g. After arrival, animals were given 5 to 8 days to acclimate to their environment. They were housed in hanging wire cages under a 12 hr light/dark cycle at 70°F and 30 to 70% relative humidity. Rats were provided standard rat chow and water *ad libitum* for the duration of each experiment.

Two experiments were conducted, noted as experiment 1 (n=16), and experiment 2 (n=12). In experiment 1, rats were treated daily for 28 days with 14 mg/kg body weight DE-71, a commercial PBDE mixture, to assess changes in the liver indicative of suppressed PEPCK and associated metabolic stress. These data served to inform experiment 2, in which rats were treated with the same amount of DE-71 for the same duration to address changes in glyceroneogenesis, hepatic lipid metabolism, and PEPCK protein.

After acclimatization, treatment was administered daily between 8:00-10:00 AM, using a standard gavage method. Animals in the treatment group (TRT) were gavaged with 14 mg/kg DE-71, while animals in the control group (CON) were gavaged with a comparable amount of corn oil vehicle. Although treatment starts dates were staggered so that 4 animals, 2 TRT and 2 CON, could be euthanized per day, each rat was treated for 28 days, fasted for days 27 and 28, and euthanized on the morning of day 29.

Tissue procurement

Animals were euthanized via CO_2 asphyxiation. Immediately post euthanasia, animals were laid on their dorsal surface, the abdomen was wiped with ethanol, and an incision was made at the base of the abdomen and extended out and along the sides of the animal. For experiment 1, upon opening of the body cavity, the diaphragm was cut allowing access to the heart, where ~5mL of blood was removed via cardiac puncture using a 5cc syringe attached to an 18-gauge, 1.5" needle. Livers were then removed, rinsed in cold water, weighed, and whole liver weight was recorded. Two-5mg samples of liver were removed and fixed in 10% formalin for later histological analysis. The rest of the liver was divided into approximate 2-gram portions, frozen in liquid nitrogen and stored at -20°C for later use.

For experiment 2, livers were removed, rinsed, weighed and three-200mg portions of each liver were removed as follows: the liver was placed on its ventral surface and the first sample was taken from the outer portion of the far left lobe (denoted "1" on figure 2). The liver was then turned over (as seen in figure 2), and the

next sample was taken from the central portion of the far left lobe (denoted “2” on figure 2). The final portion was taken from the tip of the triangular looking lobe (denoted “3” on figure 2). Liver sections were set on ice for subsequent glyceroneogenesis assay.

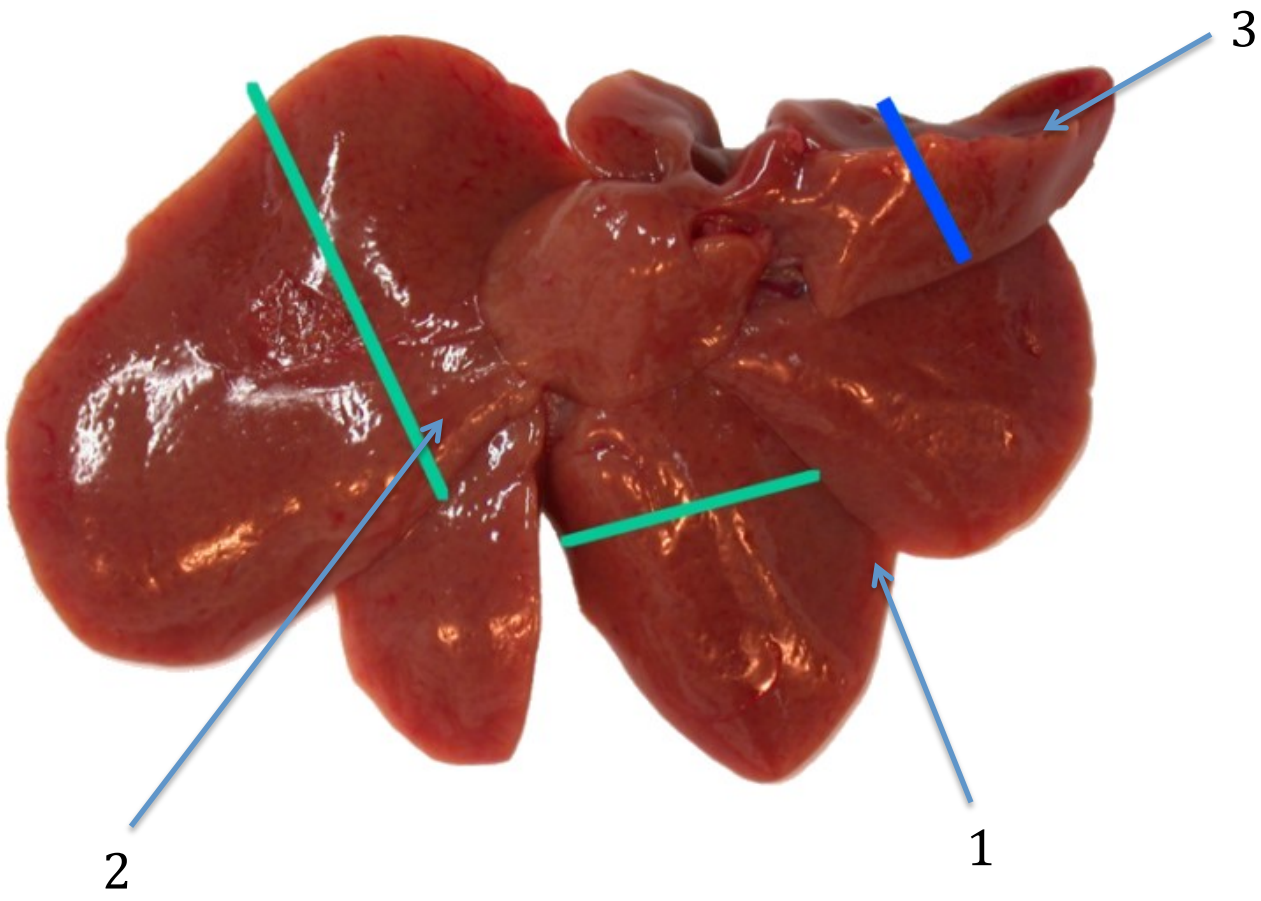

Figure 2. Ventral surface of rat liver. Location of samples removed from each liver for glyceroneogenesis quantification are indicated by respective numbers. (Picture from Ruehl-Fehlert et al., 2003).

The rest of the liver was divided into approximate 2-gram portions and immediately frozen in liquid nitrogen for later determination of PEPCK protein, PEPCK activity, and liver lipid accumulation.

Preparation of gavage solutions

For experiment 1, a 2-gram aliquot of DE-71 was obtained in an amber glass bottle from NIEHS (Lot# 1500K07A), originally obtained from Great Lakes Chemical Corporation. The bottle was stored at room temperature in a dark drawer until solution preparation. First, 1200 uL hexane was added to the amber glass bottle and stirred with a glass stir rod for approximately 10 minutes, until the sticky, viscous material was completely dissolved from the bottom, sides, and mouth of the bottle. The solution was then poured into a 150mL amber glass bottle containing 60mL corn oil. An additional 51mL corn oil was added to the bottle, which was then vortexed for 60 seconds. The hexane used to dissolve the DE-71 into solution was evaporated under nitrogen for approximately 6 hours. The final concentration of DE-71 was 2000mg/111mL, or 18mg/mL, however analysis of previous DE-71 solutions prepared following the same instructions found DE-71 concentration to be approximately 14mg/mL, suggesting that some DE-71 may be lost in preparation.

For experiment 2, DE-71 was obtained in a clear glass bottle wrapped in paper towel and tape from the University of Indiana (Lot# G550QF65A), originally obtained from Great Lakes Chemical Corporation. To obtain an approximate 2-gram portion, a small amber glass bottle and stir rod were placed on an analytical scale, which was then

zeroed. The stir rod was then used to remove a portion of the DE-71 from the clear glass bottle and transfer it to the amber glass bottle on the scale. A 1.8-gram portion was obtained, 1080uL hexane was added to the amber glass bottle, and the stir bar used to transfer the DE-71 from the original source was then used to stir the solution for approximately 10 minutes, until the DE-71 was entirely dissolved from the bottom and sides of the amber glass bottle, as well as the bottom and sides of the glass stir rod. The solution was then transferred to a 150mL amber glass bottle containing 54mL corn oil. Another 45.9mL corn oil was added to the bottle, which was then vortexed for 60 seconds. The hexane was evaporated under nitrogen for approximately 6 hours. The concentration of the solution was expected to be similar to those previously prepared by this method, 14mg/mL.

To prepare the corn oil control solution, the same preparation was used as above, excluding the addition of DE-71. For experiment 1, 1200uL hexane was added to 111mL corn oil, vortexed for 60 seconds, and hexane was evaporated. For experiment 2, 1080uL hexane was added to 99.9mL corn oil, vortexed for 60 seconds, and hexane was evaporated.

MEASUREMENTS

Serum metabolites

To analyze biochemical makers of metabolic stress that may accompany PBDE exposure, serum concentrations of a suite of metabolites were determined from rats in experiment 1. Blood was collected via cardiac puncture, transferred to 5mL serum

separator Vacuette® tubes, and left to clot at room temperature for approximately 2 hours before centrifugation at room temperature for 15 minutes at 1200 x g (3000 rpm) in an IEC – Centra8R centrifuge, to separate serum from plasma. Serum was then poured off into a plastic, 5mL storage tube and frozen at -20°C. Samples were sent to Marshfield Laboratories (Marshfield, WI) for determination of the following metabolites: serum glucose, alanine aminotransferase, alkaline phosphatase, total bilirubin, cholesterol, total protein, albumin, urea, creatinine, calcium, sodium, potassium, chloride, globulin, albumin/globulin ratio, urea/creatinine ratio, sodium/potassium ratio, beta hydroxybutyrate, triglycerides, and non-esterified fatty acids.

Histological analysis

To analyze visual changes in the liver that accompany PBDE exposure and may be indicative of metabolic stress, histological examination of livers from rats in experiment 1 was conducted. The formalin-fixed sections of each liver were sent to Dr. Roger Wells of the New Hampshire Veterinary Diagnostic Lab at the University of New Hampshire. Dr. Wells cut thin sections from each sample and mounted them on a glass slide, which he then stained with hematoxylin and eosin. He then evaluated the slides using light microscopy, providing a histopathology narrative that described the changes in liver lipid content in the TRT animals compared to CON.

PEPCK activity

To confirm findings of Nash et al. (2013) that PBDE treatment at 14mg/kg BW for 28 days suppresses hepatic PEPCK activity, frozen liver tissue was used to measure PEPCK activity using a spectrophotometric method within 3 months of euthanasia in experiment 2.

Liver cytosol extraction

Four samples were processed at a time. Two CON and two TRT samples were removed from the freezer and thawed on ice for 30-45 minutes, during which time homogenization buffer was made fresh. Once thawed, one sample at a time was weighed, hand minced with scissors, and transferred to a 50mL conical bottom screw cap tube with 9 volumes of homogenization buffer, followed by homogenization for 15 seconds with a Powerstat® polytron electric homogenizer set at 60.

Samples were centrifuged for 15 minutes at 3116.425 x g (5000 rpm) and 4°C in a Sorvall Evolution RC centrifuge. Supernatants were removed and centrifuged for 60 minutes at 59466 x g (30,000 rpm) and 4°C in a Beckman L8-80 ultracentrifuge. Glass Pasteur pipettes were used to remove the fat that had accumulated at the surface of samples, and the supernatants were transferred with plastic transfer pipettes to 15mL conical bottom screw cap tubes and placed on ice for immediate spectrophotometric analysis.

Spectrophotometric assay

Four prepared samples were kept on ice while being analyzed for PEPCK activity, one at a time. Liver cytosol containing PEPCK was combined with malate dehydrogenase (MDH), varying concentrations of malate, and NAD^+. MDH uses malate and NAD^+ to produce oxaloacetate (OAA), the substrate for PEPCK, in addition to NADH, a biochemical that can be measured spectrophotometrically at 340nm. MDH is a reversible enzyme that will reach equilibrium based on the amount of substrate available. If PEPCK activity is low and OAA is not being used, MDH will slow down its production or move the reaction in the opposite direction. NADH is made in a 1:1 ratio with OAA, so as the production of OAA is reduced, so is the production of NADH. If PEPCK activity is high and OAA is continually used, MDH will continue to make OAA, in addition to NADH. Therefore, the amount of NADH will directly reflect the activity of PEPCK in this closed system.

Each liver cytosol was assayed at 0, 0.25, 0.5, 1, 2, 4, and 8mM malate, all run in duplicate. One cuvette at a time, the following ingredients were added to a 3 mL acrylic cuvette: 330 uL ddH_2O, 300 uL 5mM $MnCl_2$, 200 uL 10mM NAD^+, 50 uL 1:50 MDH (2.2mg/mL), and varying amounts of malate and 100mM Tris (see Table 1). The volume in the cuvette after the addition of these ingredients totaled 1680 uL. The cuvette was then incubated in a 37°C water bath for 3 minutes followed by the addition of 120 uL liver cytosol and incubated for 1 minute in a 37°C water bath. The cuvette was removed from the water bath, wiped on all sides with a Kimwipe, and placed in a Milton Roy

Spectronic Genesys 5 spectrophotometer with a temperature controlled chamber set at 37°C. Finally, 200 uL 10mM GTP was added to start the reaction, bringing the final volume in the cuvette to 2 mL. The absorbance at 340nm was recorded every 15 seconds for 2 minutes and the first 4 readings were used in the final calculation of PEPCK activity.

Final Malate Concentration in Cuvette (mM)	**Malate (uL)**	**100mM Tris (uL)**
0	0	800
0.25	50[1]	750
0.5	100[1]	700
1	200[1]	600
2	400[1]	400
4	800[1]	0
8	800[2]	0

Table 1. Final concentrations and volumes of malate for PEPCK assay. [1]10mM malate stock, [2]20mM malate stock.

Solutions

CYTOSOL PREPARATION

Homogenization Buffer was prepared fresh for each set of 4 samples. The following ingredients were added, one at a time, to a 150mL glass beaker:

20mL 0.5M potassium phosphate, pH 7.0
60mL doubly distilled H_2O (ddH_2O)
5mL 20mM EDTA
200uL 0.5mM leupeptin
2mL 50mM PMSF, dropwise
2mL 50mM DTT, dropwise

The final volume was brought to 100mL with ddH2O and the solution was kept at room temperature during liver cytosol preparation.

0.5M Potassium Phosphate, pH 7.0 was made by adding 13.609 g potassium phosphate (MW=136.09 g/mol) to 150 mL ddH_2O, stirring until dissolved, adjusting pH to 7.0 with 10M NaOH, and bringing the final volume to 200 mL with ddH_2O. The solution was stored at 4°C.

20mM EDTA was made by adding 0.8089 g EDTA (MW=404.45 g/mol) to 90 mL ddH_2O, stirring until dissolved, and bringing the final volume to 100 mL with ddH_2O. The solution was stored at 4°C.

0.5mM Leupeptin was made by adding 0.0021 g leupeptin (MW=426.6 g/mol) to 10 mL ddH_2O, stirring until dissolved, and aliquoting 200 uL portions into Eppendorf tubes. Aliquots were stored at -20°C.

50mM PMSF was made by adding 0.1742 g PMSF (MW=174.19 g/mol) to 18 mL ethanol, stirring to dissolve, and bringing the final volume to 20 mL with ethanol. The solution was stored at 4°C.

50mM DTT was made by adding 0.154 g DTT (MW=154.25 g/mol) to 18 mL ddH_2O, stirring until dissolved, and bringing the final volume to 20 mL with ddH_2O. The solution was stored at 4°C.

SPECTROPHOTOMETRIC ASSAY

5mM $MnCl_2$ was made by adding 0.0989 g $MnCl_2$ (MW=197.91 g/mol) to 100 mL ddH_2O and stirring until dissolved. The solution was stored at 4°C.

10mM NAD was made by adding 0.1326 g NAD (MW=663.43 g/mol) to 20 mL ddH_2O, stirring until dissolved, and aliquotting 1.3 mL portions into Eppendorf tubes. The aliquots were stored at -20°C.

1:50 Malate Dehydrogenase (MDH) from Bovine Heart was made fresh for each set of 4 samples by adding 60 uL MDH (Sigma Aldrich, 2770 units/mg protein) to 2940 uL 0.9% NaCl, and vortexing briefly. The solution was kept on ice.

0.9% NaCl was made by adding 0.9 g NaCl (MW=58.44 g/mol) to 90mL ddH_2O, stirring until dissolved, and bringing the final volume to 100 mL with ddH_2O. The solution was stored at 4°C.

100mM Tris, pH 8.0 was made by adding 1.211 g Tris (MW=121.14 g/mol) to 80 mL ddH_2O, stirring until dissolved, adjusting the pH to 8.0 with 10M HCl, and bringing the final volume to 100 mL with ddH_2O. The solution was stored at 4°C.

10mM Malate was made by adding 0.0712 g malate (MW=178.05 g/mol) to 40 mL 100mM Tris and stirring until dissolved. The solution was stored at 4°C.

20mM Malate was made by adding 0.0712 g malate (MW=178.05 g/mol) to 20 mL 100mM Tris and stirring until dissolved. The solution was stored at 4°C.

10mM GTP was made fresh for each set of 4 samples by adding 0.0785 g GTP (MW=523.2 g/mol) to 15 mL 100mM Tris and stirring until dissolved. The solution was kept at room temperature.

Calculations

Beer's law was used to calculate activity of PEPCK using the absorbance at 340nm. The equation calculates the activity of PEPCK as a rate, using the relationship

A=Ebc, where A is absorbance at 340nm, E is the extinction coefficient of NADH (6200L/mol x cm), b is the path length of the cuvette (1 cm), and c is the concentration in mol/L. The volume in the cuvette must be accounted for, in this case 2 mL, in addition to the volume of cytosol used, which was 120 uL. The following equation can be used to express activity of PEPCK in umol/min/gram liver.

$$\frac{\left\{\left(\frac{\text{(Average A/min)}}{\text{6200 L/(mol x cm)}}\right) \times 1\text{ cm} \times 10^6\text{ umol/mol} \times 0.002\text{L}\right\}}{\left(\frac{\text{Liver (g) / buffer (mL)}}{\text{1000 ul/mL}}\right) \times 120\text{ uL}}$$

PEPCK protein determination

To determine if the PBDE-driven suppression in PEPCK activity is due to a reduction in PEPCK protein, western blotting methods were used in experiment 2. Protein was extracted from liver samples stored frozen for approximately 1 week.

Protein extraction

Four samples were processed at a time. Liver samples were thawed, and approximately 5mg tissue was dissected from each sample and placed into a 5 mL plastic scintillation vial with 300 uL lysis buffer. Each sample was homogenized for approximately 10 seconds with a Powerstat® polytron electric homogenizer set at 60.

The blades of the homogenizer were washed with 600 uL lysis buffer into the cuvette containing the sample, which was then transferred to a 1.5 mL Eppendorf tube. Eppendorf tubes were maintained at a constant agitation on an orbital shaker for 2 hours at 4°C (in a walk-in refrigerator). The samples were then centrifuged for 20 minutes at 16,000 x g at 4°C in an Eppendorf 5418R tabletop centrifuge. The supernatant was transferred into a clean Eppendorf tube using a 5 mL plastic transfer pipette. Samples were kept on ice for immediate protein quantification using a commercial DC protein kit (BioRad, Cat. No. 500-0112), and then frozen overnight for use the next morning.

Western blot

A volume of sample equivalent to 25 ug total protein was mixed in a 3:1 ratio with 4X Laemmli sample buffer and boiled for 3 minutes at approximately 100°C. Immediately after boiling, sample was loaded into a mini-protean TGX pre-cast 12-well gel (BioRad, Cat. No. 456-9035). A protein plus dual color standard ladder (10-250 kD, BioRad, Cat. No. 161-0374) was loaded into the first and last wells of each gel to provide a molecular ladder as a point of reference. The second and eleventh wells contained a positive control of rat liver extract (Santa Cruz, Cat. No. SC-271029). Wells 3-10 contained liver samples, in duplicate. A diagram of each gel was recorded, noting how much sample, ladder, or positive control was added to the wells. Each gel was then designated a number, and the numbers referred to the placement order of the gels in

the electrophoresis cabinet. From the back of the cabinet to the front, the gels were numbered 1, 2, and 3, and these numbers were indicated on the gel diagrams.

Gels were then placed in the electrophoresis cabinet containing approximately 1 liter of 1x tris-glycine/SDS running buffer. The cabinet was attached to a power source set to 175 volts of electricity for approximately 45 minutes, allowing for the protein to run down the gels and separate by size, with the largest proteins separating out first.

When the samples had run to the bottom of the gel, gels were removed from the running buffer. The gels were removed from their outer plastic casing by forcing open the plastic casing using the gel opening fork at the specified arrows. Once removed, the bottom edge of each gel was cut off using a razor blade, and finally, gels were placed in a bucket filled with approximately 1 L of 1x tris-glycine transfer buffer. Gels were placed in the buffer and assembled in a transfer sandwich (described below) one at a time, to ensure the identity of each gel was maintained.

Plastic cassettes were used to assemble transfer sandwiches. These cassettes allow for the gels to be held in tight, close proximity to Immunoblot PVDF membranes (BioRad, Cat. No. 162-0174), allowing for protein to transfer from the gels to the membranes which would next be incubated with antibodies. One membrane at a time was first incubated in methanol for 1 minute followed by pre-incubation in 1x transfer buffer in a 5-liter plastic tub for 5 minutes. The membrane was then labeled, according to which gel it would be incubated with. Once labeled, the membrane was placed into the plastic tub containing a liter of transfer buffer along with the cassette, 2 foam sponges, 2 transfer papers, and its corresponding gel. The sandwich was assembled

starting with the black side of the cassette, followed by a sponge, a piece of transfer paper, the gel, with lane 1 on the left side, membrane, another piece of transfer paper, the other sponge, and finally the clear side of the cassette. After removal of all bubbles from the sponges and from between the membrane and gel, the two white clips were slid onto the top of the transfer sandwich to hold it together. Once one sandwich was assembled, it was kept in the plastic tub containing the transfer buffer to avoid drying out of the membrane, a key concern at all points of the procedure.

Once all three sandwiches were assembled, the first two were placed into one electrophoresis cabinet containing one liter of 1x transfer buffer, and the third was placed into a separate electrophoresis cabinet containing one liter of 1x transfer buffer. An ice pack was added to the front of each cabinet along with a magnetic stir bar. The cabinets were then placed on a large stir plate, allowing for constant stirring of the transfer buffer overnight, while the cabinets were attached to a power source set to 30 volts of constant power.

Approximately 21 hours after start of the transfer process, the cabinets were disconnected from the power supply and the contents of the cabinets were emptied back into the plastic tub that was originally used for cassette assembly. Once in the bucket, sandwiches were disassembled and membranes were immediately transferred to individual small dishes containing phosphate buffered saline (PBS) solution with 10% w/v non-fat dry milk and 1:500 dilution PEPCK-specific primary antibody (Santa Cruz, Cat. No. SC-271029). After 1-hour incubation with primary antibody, the membranes were washed three times for 10-minute increments in PBS containing 10% non-fat dry

milk. After washing, the membranes were incubated for another 1-hour period in a light sensitive goat anti-mouse IgG secondary antibody (Licor, Cat. No. 827-08364), at a 1:15,000 dilution, according to manufacturer instructions. The membranes were once again washed three times for 10-minute increments to remove any excess, unbound secondary antibody. The secondary antibody bound to primary antibody, providing a fluorescent tag that was then visualized using a Li-Cor Odyssey scanner.

To visualize PEPCK on the membranes, the Li-Cor Odyssey scanner was used with all lights turned off and room shades closed. Membranes were placed one at a time, face down on the front left corner of the scanner. Bubbles were then pressed out from under the membrane using a 3-inch rubber roller, a rubber cover was placed on top of the membrane, and the scanner cover was closed. The scanner was then instructed to visualize the membrane, producing a picture that was sent to the computer and saved as a .tif file to a USB drive. This process was repeated for all 3 membranes. Pictures were then used to calculate density of each PEPCK band on the 3 membranes using the Un-Scan-It computer densitometry program. This provided semi-quantitative data regarding overall PEPCK protein present in the samples.

Solutions

Homogenization Buffer was made by adding the following ingredients to a half liter glass bottle in the order listed:

12.5 mL 1M HEPES
2.2 g NaCl
0.105 g NaF
0.5 mL 500mM EDTA

25 mL glycerol
1.25 mL Triton X-100
Bring the final volume to 250 mL using ddH_2O

The solution was made the day prior to protein extraction and stored at 4°C for approximately 2 weeks.

Lysis Buffer was made by placing 15 mL homogenization buffer into a 20 mL glass beaker and adding 150 uL aprotinin (Sigma Aldrich, Cat. No. A6279, 3-7 TIU/mg protein) and 150 uL 1M benzamidine. Buffer was kept on ice for the duration of the protein extractions.

1M HEPES was made by adding 3.098 g HEPES (MW=238.3 g/mol) to about 10 mL ddH_2O, stirring until dissolved and bringing final volume to 13 mL with ddH_2O.

1M Benzamidine was made by adding 0.018 g benzamidine (MW=120.15 g/mol) to 150uL ddH_2O and mixing well until dissolved. The solution was immediately added to the lysis buffer.

4X Laemmli Buffer was combined with 2-mercaptoethanol per manufacturer instruction (BioRad, Cat. No. 161-0737).

Running Buffer (tris-glycine/SDS) was made by adding 100 mL 10X tris-glycine/SDS (BioRad, Cat. No. 161-0732) to 900 mL ddH_2O and mixing well. Buffer was made the morning of use and was stored at 4°C until needed.

Transfer Buffer (tris-glycine) was made by adding 200 mL methanol to 700 mL ddH_2O, followed by the addition of 100 mL 10X tris-glycine (BioRad, Cat. No. 161-0734). The solution was then mixed well. Buffer was made the morning of use and was stored at 4°C until needed.

Phosphate-Buffered Saline (PBS) was made by adding 100 mL 10x-PBS (BioRad, Cat. No. 161-0780) to 900 mL ddH_2O and mixing gently. Buffer was made the morning of use and was stored at 4°C until needed.

Glyceroneogenesis

To address the hypothesis that PBDE treatment at 14 mg/kg BW for 28 days suppresses hepatic glyceroneogenesis, fresh liver tissue was used to quantify hepatic glyceroneogenesis using a radioactive method in experiment 2.

Glyceroneogenesis samples were transported back to the lab on ice, where each of the 3 samples was placed in 1 well of a 6-well plate. Each well had 1.5mL Kreb's-Ringer-Bicarbonate buffer (KRB) containing 5mmol glucose. Holding each sample above its well, it was cut in ~10, 20mg pieces using tweezers and small dissecting scissors. Each well was gassed with 95% CO_2, 5% O_2 and incubated on a shaker at 37°C for 6 hours.

Approximately 30 minutes before the end of incubation, the radioactive working solution was made. Once the 6-hour incubation was complete, a Pasteur pipette was used to remove the KRB from each well, followed by addition of 1.5mL working solution to each well. Wells were then gassed with 95% CO_2, 5% O_2 and incubated on a shaker for 2 hours at 37°C, allowing for incorporation of ^{14}C-pyruvate into the glycerol backbone of triglycerides in the liver tissue. At the end of this incubation period, a Pasteur pipette was used to remove the radioactive working solution from each well, and wells were filled with cold KRB, halting metabolism of the tissues. The KRB was removed using 5mL plastic syringes, and then 1.5mL phosphate-buffered saline (PBS) was added to

each well for washing purposes. Each sample set was then transferred to another 6-well plate containing 1.5mL PBS per well. The plate was agitated lightly, followed by transfer of samples to another plate with clean PBS. This was repeated four times total, allowing for an initial PBS wash in the incubation plates, followed by four consecutive washes in clean 6-well plates. After washing was complete, each sample was removed from its well and placed in a 1.5mL Eppendorf tube, ensuring all pieces of sample congregated at the bottom of the tube. Tubes were then snap frozen in liquid nitrogen and placed in a -20°C freezer for later fat extraction.

Three-50uL aliquots of the extra working solution were removed and counted for determination of specific activity after each set of samples was incubated and frozen. Each aliquot was placed into an individual plastic scintillation vial, followed by immediate addition of 3 mL Optiphase Supermix scintillation cocktail. Vials were labeled and counted on the scintillation counter to quantify disintegrations per minute in each sample, which was then used to calculate specific activity of the working solution.

Extraction of fat for radioactive quantification

Within 3-4 weeks of initial sample incubation and freezing, fat was extracted and radioactivity incorporated into fat was quantified as a marker of glyceroneogenesis. The three samples from one animal were removed from the freezer and transferred, frozen, from the base of the eppendorf tubes into three respective glass homogenizing tubes, each containing 1 mL ddH_2O. Each sample was homogenized 6 times up and down using a hand drill and homogenizing pestle, and then transferred into a 15 mL capped-

glass centrifuge tube containing 0.25 mL chloroform. Samples were mixed by hand briefly and then transferred back to their individual homogenization tubes where they were homogenized three more times up and down. Samples were transferred back to the capped-glass centrifuge tubes, and 3.75 mL methanol:chloroform 2:1 was added. Every step was completed on ice, in the hood. Tubes were then capped and vortexed for 30 seconds before shaken mildly on ice for 30 minutes.

After 30 minutes of incubation, samples were taken off the shaker and placed on ice in the hood, where 1.25 mL chloroform was added to each tube before re-capping and mild shaking on ice for another 10 minutes. At the end of the second incubation, samples were taken off the shaker once again and placed on ice in the hood, where 1 mL ddH_2O was added to each tube before re-capping and shaking on ice for an additional 10 minutes. At the end of the final 10-minute incubation, samples were balanced against water and centrifuged at 478 x g (3000 rpm) for 15 minutes at 4°C in a Sorvall Evolution RC centrifuge. After centrifugation, 2-1 mL portions of the bottom, chloroform layer from each sample were removed and transferred into individual 5 mL plastic scintillation vials, immediately followed by the addition of 3 mL Optiphase Supermix scintillation cocktail. Vials were labeled and counted on the scintillation counter to quantify disintegrations per minute within each sample, which was then used to calculate the rates of glyceroneogenesis.

Extractions were overlapped to optimize time spent on the procedure; however only 3 sets of triplicate samples could be run at once. The second set of samples was not removed from the freezer until the timer for the first set read 13 minutes remaining

for the 30-minute incubation. Similarly, the third set was removed from the freezer when the timer for the second set read 13 minutes remaining for the 30-minute incubation. This was to ensure that at the end of the third incubation, the samples could go directly into the centrifuge without any lag time. Preliminary studies revealed that a lag between incubation and centrifugation caused a dramatic drop in radioactivity, skewing the data. It was also important to remove the 2-1 mL aliquots from each sample tube within the first 2 minutes of removal from the centrifuge, to ensure that the aliquots reflected optimal separation of fat from other components of the liver samples. If this transfer took any greater than 2 minutes, the top layer started to fall back into the bottom layer, causing a distinct difference in radioactivity between the first and third triplicate samples.

Solutions

Kreb's-Ringer-Bicarbonate Buffer (KRB) was made by adding the following amounts of each stock solution in the order listed, and stored at 4°C for up to 1 week:

500 mL ddH_2O
25 mL 1M HEPES
62.5 mL 2M NaCl
5 mL 1m KCl
1 mL 1M KH_2PO_4
1.25 mL 1M $MgCl_2$-$6H_2O$
1.25 mL 1M $CaCl_2$-$2H_2O$
25 mL 1M $NaHCO_3$
pH to 7.4, bring to final volume of 1 Liter with ddH_2O

Stock solutions were made as follows and stored at 4°C for approximately 6-8 weeks:

1M HEPES was made by adding 119.15 g HEPES (MW=238.3 g/mol) to about 450 mL ddH_2O and stirring until dissolved. The pH of the solution was adjusted to 7.76 and the final volume of the solution was brought to 500 mL with ddH_2O.

2M NaCl was made by adding 58.44 g NaCl (MW=58.44 g/mol) to approximately 450 mL ddH_2O, stirring until fully dissolved, and bringing the final volume to 500 mL with ddH_2O.

1M KCl was made by adding 7.46 g KCl (MW=74.6 g/mol) to approximately 90 mL ddH_2O, stirring until fully dissolved, and bringing the final volume to 100 mL with ddH_2O.

1M KH_2PO_4 was made by adding 13.609 g KH_2PO_4 (MW=136.09 g/mol) to approximately 90 mL ddH_2O, stirring until fully dissolved, and bringing the final volume to 100 mL with ddH_2O.

1M $MgCl_2$-$6H_2O$ was made by adding 20.33 g $MgCl_2$-$6H_2O$ (MW=203.30 g/mol) to approximately 90 mL ddH_2O, stirring until fully dissolved, and bringing the final volume to 100 mL with ddH_2O.

1M $CaCl_2$-$2H_2O$ was made by adding 14.702 g $CaCl_2$-$2H_2O$ (MW=147.02 g/mol) to approximately 90 mL ddH_2O, stirring until fully dissolved, and bringing the final volume to 100 mL with ddH_2O.

1M $NaHCO_3$ was made by adding 42.005 g $NaHCO_3$ (MW=84.01 g/mol) to approximately 450 mL ddH_2O, stirring until dissolved, and bringing the final volume to 500 mL with ddH_2O.

^{14}C-pyruvate was ordered from Perkin Elmer (Cat. No. NEC2550, 50 uCi) in powder form. To reconstitute into solution, 2 uL ddH_2O was added for every uCi of radioactivity present.

Working Solution was made fresh for each set of 4 livers (liver samples were run in triplicate; working solution made for 12 samples at a time). First, 19 mL cold KRB was added to a 50 mL glass beaker. The beaker was placed on a heating stir plate followed by the addition of 10.45 mg pyruvic acid and a magnetic stir bar. Solution was stirred until the pyruvic acid dissolved, followed by addition of 380 mg fatty acid free bovine serum albumin (FAF-BSA) (Sigma, Cat. No. A7030). The hot plate was turned on low and stirring was continued until FAF-BSA was completely dissolved. Hot plate was then turned off while stirring was continued for the final addition of 38 uL ^{14}C-pyruvate (or 1 uCi ^{14}C-pyruvate per mL working solution). The final working solution was stirred for an additional 5 minutes to ensure mixing.

Phosphate-Buffered Saline (PBS) was made by adding 100 mL 10x-PBS (BioRad, Cat. No. 161-0780) to 900 mL ddH_2O and mixing gently. The solution was stored at 4°C for approximately 3 weeks.

Methanol:Chloroform 2:1 was made by adding 90 mL methanol to a 150 mL amber glass bottle, followed by the addition of 45 mL chloroform. The mixture was then vortexed for 15-30 seconds, capped, and stored under the hood.

Calculations

Glyceroneogenesis Rate of each sample was expressed as pmol ^{14}C-pyruvate incorporated into triglyceride per hour per mg tissue (pmol/hr/mg). Specific activity (SA) was calculated every time fresh working solution was made, and was used to convert dpm into nmol per mL, because 1mL of the chloroform layer was counted at a time. The chloroform layer was approximately 2.5mL per sample, so multiplication by 2.5 allowed for the number to be expressed in nmol/whole sample. Amount of time in incubation and sample weight were also accounted for to express glyceroneogenesis as a rate in nmol/hr/mg tissue. The final rate was multiplied by 1000 to express the rate in pmol/hr/mg tissue. The following equation is a mathematical representation of the calculation used:

$$\frac{1000 \text{ pmol/nmol} * \{(\text{dpm of sample}/\text{SA of working solution in dpm/nmol}) * 2.5\text{mL/sample}\}}{(2 \text{ hours per incubation} \times \text{sample weight in mg})}$$

Each sample was counted in duplicate, and each animal had triplicate tissue samples analyzed. The duplicate rates were averaged for a within sample mean. The triplicate means were then averaged for a within animal mean. The within animal means were then averaged for a within treatment group mean.

Specific activity (SA) was calculated using the specific activity of the stock solution of ^{14}C-pyruvate, which was 9.5mCi per mmol for a bottle containing 50uCi. This corresponds to .005mmol of radioactive pyruvate in the stock solution. Working solution is made by adding 19uCi of ^{14}C-pyruvate, which is 38% of the total stock, containing

.00199mmol of radioactive pyruvate, or 1.99umol. The addition of 10.45mg cold pyruvate added 118.74umol cold pyruvate, for a total of 120.74umol pyruvate in 19mL working solution. Three aliquots of 50uL were counted of each working solution, which were then averaged to provide one value representing dpm/50uL, which was then used to calculate SA for each sample using the following mathematical relationship:

$$\frac{\text{dpm}}{0.050\text{mL}} \times \frac{19\text{mL}}{120.74\text{umol}} = (\text{dpm/umol}) \times 1000 = \text{dpm/nmol}$$

SA was calculated separately for each working solution that was made, and applied to the corresponding samples when calculating glyceroneogenesis rates.

Liver lipid content

To evaluate PBDE-associated changes in hepatic lipid content, triglycerides were extracted from frozen livers of rats in experiment 2. Liver portions were allowed to thaw, three at a time, on ice for approximately 30-60 minutes. At room temperature, three 50 mg portions of each liver were weighed out, weights recorded, and samples individually homogenized ten times up and down in 0.3 mL cold PBS. The solution was left to rest for 15 seconds followed by homogenization 5 additional times up and down. Each sample was then transferred to an individual clean, 15 mL Corex glass tube. To ensure as much sample transfer as possible, 2 mL hexane:isopropanol (3:2) solution was added to the homogenization tube, mixed lightly by hand and transferred to the Corex tube containing the sample. Each sample was then gassed with nitrogen and vigorously shaken for 1 hour. Next, 0.6 mL 0.5M sodium sulfate was added to each sample. Tubes

were then vortexed for 60 seconds, and vigorously shaken for an additional 15 minutes. After the final shake period, samples were balanced against water and centrifuged for 10 minutes at 871 x g (2700 rpm) and 23°C in a Sorvall Evolution RC centrifuge. Immediately following centrifugation, 1-1 mL aliquot of the upper phase from each sample was removed and placed in a dry, pre-weighed disposable glass tube. The samples were then dried under nitrogen gas for approximately 20 minutes and weighed again immediately, and then once more the following day to confirm complete drying. The change in weight of the tube was then used to calculate the percentage of lipid present in each liver.

Solutions

Phosphate buffered saline (PBS) was made by adding 10 mL 10x-PBS (BioRad, Cat. No. 161-0780) to 90 mL ddH_2O and mixing gently. The solution was stored at 4°C for approximately 3 weeks.

Hexane:Isopropanol (3:2) was made by adding 60 mL hexane to an amber glass bottle under the hood, followed by adding 40 mL isopropanol, capping, and vortexing lightly for approximately 15-30 seconds. The solution was stored under the hood.

0.5M sodium sulfate was made by placing 7.102 g sodium sulfate (MW=142.04 g/mol) in ddH_2O and bringing the final volume to 100 mL. The solution was mixed on a stir plate using a magnetic stir bar for approximately 5-10 mintues. The solution was stored at 4°C for approximately 3 weeks.

Calculations

The following calculation was used to determine hepatic lipid percentage:

{ 6/5* x [(final tube weight – initial tube weight) /initial weight of sample] }x 100

*6/5 is a correction factor for volume of hexane. The lipid is collected in the hexane layer, and 2 mL of 3:2 hexane:isopropanol is added to each tube, equaling a theoretical volume of 1.2 mL hexane. Only 1 mL of this is extracted and used in the final step of the method, and therefore, to account for the amount of lipid extracted in the whole volume of hexane, the raw calculated values are multiplied by (1.2/1) or (6/5).

Samples were run in triplicate, therefore three lipid percentages were calculated for each liver. Coefficient of variation (CV) was conducted within the three samples for each liver, and the data was rejected if the CV was greater than 25%. In these cases, three additional samples were taken from the liver and the method was repeated.

STATISTICS

Coefficient of variation of 25% for PEPCK activity calculated from the literature (Chauvin et al., 1996) requires 8 rats per group to detect a 45% treatment effect (Berndtson, 1991). Based on this calculation, 16 animals were used for experiment 1, n=8 per group. Coefficient of variation of 10% calculated from pilot studies for

glyceroneogenesis requires 6 rats per group to detect a 20% treatment effect (Berndtson, 1991). Based on this calculation, 12 animals were used for experiment 2, n=6 per group.

Two-way ANOVA was used to determine the effect of treatment and experiment date on body and liver weight outcomes using JMP Pro11.

Unpaired t-tests were used to compare means for CON and TRT groups for blood metabolites, PEPCK protein density, glyceroneogenesis, and liver lipid percentage using GraphPad InStat 3. Equal population standard deviations were assumed in all tests.

CHAPTER 3

PBDE-INDUCED SUPPRESSION OF PHOSPHOENOLPYRUVATE CARBOXYKINASE (PEPCK) DECREASES HEPATIC GLYCERONEOGENESIS AND DISRUPTS HEPATIC LIPID HOMEOSTASIS

INTRODUCTION

Polybrominated diphenyl ethers (PBDEs) are a class of environmental chemicals added to consumer products starting in the 1970s to help reduce flammability (Watkins et al., 2011, Besis and Samara, 2012). PBDEs have been used in a wide variety of products, including but not limited to electronics, textiles, curtains, couches and many other types of home and office furniture and upholsteries (Harrad et al., 2008, Jones-Otazo et al., 2005, Wilford et al., 2005).

Because PBDEs are added, not bound, to the products in which they are used, they freely migrate into the air and settle into the environment (Costa et al., 2008). When consumer products containing these chemicals are disposed of, either in landfills or through incineration, PBDEs will settle into sediment, sludge, and soil, where they

can contaminate the water and food supply and eventually biomagnify up the food chain (Osako et al., 2004, Hale et al., 2008, Costa et al., 2008).

The main routes of human exposure to PBDEs include inhalation and ingestion, with sources coming mainly from dust (Harrad et al., 2008), but also food sources such as fish, dairy, and meat (Costa et al., 2008). Once in the body, PBDEs tend to reside in the fat tissue due to their lipophilicity (Johnson-Restrepo et al., 2005), however metabolism of PBDEs occurs in the liver (Stapleton et al., 2009), suggesting these two tissues bear the bulk of the PBDE exposure burden.

Although PBDEs have been phased out of production since late 2013, they still persist in the environment. Homes and offices have furniture and upholsteries containing PBDEs, and disposal of these products continue to contaminate both indoor and outdoor environments.

Once inside the body, PBDEs are known endocrine disruptors. Due to the similarity in structure between PBDEs and thyroxine, PBDEs are able to competitively bind thyroid receptors α and β (Meerts et al., 2000), thyroid transporter transthyretin (Hamers et al, 2006, Marchesini et al., 2008), and effectively decrease circulating levels of the active form of thyroid hormone, triiodothyronine (Lee et al., 2010, Tseng et al., 2008). PBDEs have also been found to bind receptors for estrogen, progesterone, androgens, and glucocorticoids (Hamers et al., 2006), disrupting endocrine signaling and potentially creating obesogenic or diabetic effects (Feo et al., 2013).

In addition to endocrine-disruption, PBDEs largely affect the liver by increasing oxidative stress and antioxidant enzyme activity (An et al., 2010, Albina et al., 2010),

increasing fatty deposition in the liver (Bruchajzer et al., 2010), and decreasing activity of a key metabolic enzyme, phosphoenolpyruvate carboxykinase (PEPCK). Indeed, Nash et al. (2013) found that hepatic PEPCK activity was suppressed by 43% when male Wistar rats were exposed to 14mg/kg/day DE-71, a commercial PBDE-mixture, for 28 days. This change in enzyme activity was accompanied by an increased glucose:insulin ratio, suggesting metabolic perturbations indicative of insulin resistance.

PEPCK catalyzes the conversion of oxaloacetate (OAA) to phosphoenolpyruvate (PEP), a regulated and crucial beginning step of both *de novo* glucose synthesis via gluconeogenesis, and triglyceride resynthesis via glyceroneogenesis (Yang et al., 2009). Increased enzyme activity is necessary for these pathways to be robust during fasting, and the primary mechanism for controlling PEPCK activity is via increased transcription (Chakravarty et al., 2005, Yang et al., 2009).

Reduced PEPCK activity has been associated with physiological consequences, such as decreased hepatic gluconeogenesis (Zhang et al., 2012, Diani-Moore et al., 2013) and changes in glucose:insulin ratio (Nash et al., 2013). These findings suggest decreased PEPCK activity may be associated with perturbed hepatic carbohydrate metabolism. Less explored is how changes in PEPCK may be affecting glyceroneogenesis and consequently, hepatic lipid metabolism. Because glyceroneogenesis generates glycerol-3-phosphate, the necessary backbone for fatty acid esterification, disruption of this pathway could lead to decreased triglyceride formation and increased hepatic and systemic fatty acid levels. Chronically high levels of fatty acids have been shown to perturb insulin signaling, leading to the development

of insulin resistance and playing a potential role in the development of diabetes. Thus, the goal of the current study was to examine PBDE-induced alterations of hepatic glyceroneogenesis and PEPCK expression, and the resulting implications for hepatic lipid metabolism.

MATERIALS AND METHODS

Animals

Twenty-eight weanling male Wistar rats (Charles River Laboratory, Wilmington, MA) were used for this study. Rats weighed between 75-100 g at arrival and were allowed to acclimate to their new environment for 5-8 days. They were housed individually in stainless steel hanging basket cages under a 12 h light/dark cycle and fed standard rat chow and water *ad libitum*. Procedures and methods were approved by the University of New Hampshire Institutional Care and Use Committee (#131003 and #14071).

Chemicals

DE-71 was generously donated from NIEHS (Lot# 1500K07A) and Indiana University (Lot# G550QF65A). Approximately 2 grams were dissolved in hexane and corn oil; excess hexane was evaporated under nitrogen for a final PBDE concentration of 14 mg/mL. Control solution was prepared with identical amounts of hexane using the same procedure, without the addition of DE-71.

Treatment

All rats were gavaged daily with 14 mg/kg body weight DE-71 (n=14, TRT) or a comparable amount of corn oil vehicle (n=14, CON) between 8:00-10:00 AM, for 28 days. On days 27 and 28, rats were fasted and then euthanized between 8:00-10:00 AM on the morning of day 29. Rats were weighed every 3 days throughout the experiment. The study included two experiments with identical treatment methods conducted nine months apart, using lot #1500K07A for the first experiment and lot #G550QF65A for the second experiment.

Tissue Procurement

After the 48-hour fast, rats were weighed then euthanized via CO_2 asphyxiation. Three to five mL of blood were collected immediately via cardiac puncture, followed by removal of the liver. Livers were rinsed, blotted dry, and weighed. Each liver was separated into two 5 mg-portions that were fixed in formalin for histological analysis, three 200 mg-portions that were placed on ice for glyceroneogenesis measurements, and three to five 2 gram-portions that were snap frozen in liquid nitrogen and stored at -20°C for later quantification of PEPCK protein, PEPCK activity, and hepatic lipids.

Serum Metabolites

Blood was allowed to clot at room temperature for approximately 2 hours, and then centrifuged at room temperature for 15 minutes at 1200 x g. Serum was separated and

frozen at -20°C, until analysis by Marshfield Laboratories (Marshfield, WI) for blood metabolites.

Histological Analysis

Formalin-fixed livers were sectioned, mounted on glass slides and stained with hematoxylin and eosin for evaluation of lipid content using light microscopy by the NH Veterinary Diagnostic Lab at the University of New Hampshire.

PEPCK Protein

Liver was thawed on ice and protein was extracted from a 5 mg-portion by homogenization in 300 uL of lysis buffer containing 50mM Hepes, 150mM NaCl, 10mM NaF, 1mM EDTA, 10% glycerol, 0.5% Triton X-100, 1% aprotinin (3-7 TIU/mg protein) and 10mM benzamidine. The blade was rinsed with 600uL lysis buffer, which was added to the sample, and samples were maintained at a constant agitation on an orbital shaker for 2 hours at 4°C. Finally, samples were centrifuged for 20 minutes at 16,000 x g and 4°C. Supernatant was assayed for protein (DC protein kit, BioRad), and frozen overnight for use the next morning.

Twenty-five ug protein from each sample was loaded in duplicate onto mini-protean pre-cast gels (BioRad) and separated via 10% SDS-PAGE before transfer onto Immuno-blot PVDF membranes (BioRad). Membranes were incubated for one hour with a mouse PEPCK primary antibody, 1:5000 dilution (Santa Cruz Biotechnology, Dallas, TX), washed with PBS containing 10% nonfat dry milk to remove excess unbound antibody, incubated for one hour with a light-sensitive goat anti-mouse IgG

secondary antibody (LiCor), and washed with PBS containing 10% nonfat dry milk. Gels were visualized using a Li-Cor Odyssey Scanner and semi-quantified using densitometry (Un-Scan-It).

PEPCK Activity

Enzyme activity was measured as previously described (Nash et al., 2013) with modifications. Approximately 2-gram portions of each liver were homogenized and centrifuged at 3116.425 x g (5000 rpm) for 15 minutes at 4°C, and the cytosolic fraction was isolated by centrifugation at 59466 x g (30,000 rpm) for 60 minutes at 4°C. PEPCK activity was measured in a 3 mL cuvette with final concentrations of 50mM Tris, 0.75mM $MnCl_2$, 1mM NAD^+, 6 units MDH, 1mM GTP, and 0-8 mM malate (final volume was 2 mL) as follows: the cuvette was incubated for 3 minutes at 37°C containing double-distilled water, $MnCl_2$, NAD^+, MDH, malate and Tris, pH 8.0; cytosol was added and incubation continued for another minute; GTP was added to start the reaction. The samples were read at 340nm every 15 seconds for 2 minutes, and the average ΔOD was calculated for the first minute. Samples were run in duplicate with 0, 0.25, 0.5, 1, 2, 4, and 8mM malate.

Hepatic Lipids

Livers were thawed on ice and lipids extracted as described by Nash et al. (2013).

Hepatic Glyceroneogenesis

Hepatic glyceroneogenesis rates were measured as described previously (Jaubert et al., 2012) with modifications. In brief, each of three 200 mg-portions of liver was cut into approximately 10 pieces, and placed in one well of a 6-well plate containing 1.5 mL Krebs Ringer bicarbonate buffer containing 5mM glucose. Samples were incubated for 6 hours at 37°C, followed by removal of media using glass Pasteur pipette. Each well was then incubated in 1.5mL Krebs Ringer bicarbonate buffer containing 6.25 mM pyruvic acid, 2% fatty acid free BSA, and 1.5 uCi ^{14}C-pyruvate at 37°C. After 2 hours, samples were rinsed 6 times in cold PBS, placed in 1.5mL Eppendorf tubes, snap frozen in liquid nitrogen, and stored at -20°C for up to 2 weeks. Fat was extracted from frozen samples by the following steps, all on ice: each sample was homogenized in 1mL double distilled water for 5 strokes, 0.25mL chloroform was added and sample homogenized for 3 strokes, 3.75 mL methanol:chloroform 2:1 was added and sample shaken for 30 minutes. Next, 1.25mL chloroform was added and the sample was shaken for 10 minutes, followed by the addition of 1 mL ddH_2O and 10 minutes of shaking. The samples was centrifuged for 15 minutes at 478 x g and 4°C, and two 1mL-portions of the bottom phase of each sample were removed and counted in a scintillation counter to calculate incorporation of ^{14}C-pyruvate into hepatic lipids.

Statistics

A two-way ANOVA was used to evaluate the effect of treatment and time of experiment on body weight and liver weight. Means for CON and TRT groups for blood metabolites, hepatic PEPCK Vmax and Km, hepatic lipids, hepatic glyceroneogenesis, and hepatic PEPCK protein were compared using unpaired t-tests, assuming equal population standard deviations using GraphPad InStat3 and JMP Pro 11. Significance was set as $P<0.05$.

RESULTS

Animal and Liver Measurements

Analysis of final body weight, liver weight, and liver as a percent of body weight for rats in both experiments revealed no effect of time of experiment, but a significant effect of treatment (Table 2). DE-71 treatment increased liver weight by 33% and liver weight as a percent of body weight by 26%, but did not have an effect on final body weight. Furthermore, DE-71 treatment increased hepatic concentrations of BDE-47, BDE-99, and BDE-100 by 59-, 31-, and 80-fold, respectively (Table 3).

Hepatic PEPCK Activity

Hepatic PEPCK activity from CON vs. TRT rats demonstrates a 28% decrease of activity in livers from TRT rats compared to CON at the highest substrate concentration of 8mM (Figure 2). Kinetics curves of PEPCK activity from individual rat livers were plotted on Sigma Plot 12, and a hyperbolic curve was fit to the data and used to determine individual hepatic PEPCK Km and Vmax, revealing a 40% decrease in Vmax

of TRT animals compared to CON, with no change in Km between treatment groups (Table 4).

Hepatic PEPCK Protein Levels

A representative Western blot of hepatic PEPCK protein levels in TRT and CON samples is shown in Figure 4. Quantification of the data (n=6 per group) using densitometry revealed a 17% decrease in PEPCK protein in livers of TRT rats compared to CON ($p=0.11$). A Q-test revealed no clear outliers due to the limited sample size; however samples that skewed coefficient of variation by greater than 25% were removed from the comparison. Removal of one CON and one TRT point tightened coefficient of variation by 34% and 28%, respectively, and comparisons of the new means revealed a significant, 23% decrease in PEPCK protein in livers of TRT animals compared to CON ($p<0.05$, $n=5$).

Blood Metabolites

To evaluate if PBDE-induced PEPCK suppression affected hepatic gluconeogenesis, serum glucose was measured. TRT animals exhibited a 48% reduction in serum glucose compared to CON, after a 48-hour fast (Table 5). Beta-hydroxybutyrate, a marker of excess unesterified fatty acid metabolism, was significantly increased by 27% in TRT animals compared to CON ($p<0.05$). This was accompanied by a significant 27% reduction in serum triglycerides in TRT animals. Serum NEFA and cholesterol levels were not different between the two groups.

Hepatic Lipid Content

Hepatic lipid was 29% lower in livers from TRT animals compared to CON ($p<0.05$, Figure 5). In contrast, histological data illustrated mild lipid vacuolation in the midzonal region of livers from 7 of the 8 TRT rats, and 0 of the 8 CON rats (Figure 6).

Hepatic Glyceroneogenesis

There was a significant, 41% decrease in hepatic glyceroneogenesis in livers of TRT animals compared to CON (Figure 7). The change in glyceroneogenesis was not dependent on liver location because triplicates were run from three distinct areas of each liver and there were no significant differences between triplicate samples within each treatment group.

DISCUSSION

This study is the first to evaluate hepatic lipid metabolic perturbations caused by the commercial PBDE-mixture, DE-71, revealing that PBDEs suppress hepatic glyceroneogenesis *in vitro*. This suppression is consistent with our findings of reduced hepatic PEPCK protein and activity. To our knowledge, this is the first study to (1) address hepatic glyceroneogenesis in response to PBDE exposure, and (2) illustrate a relationship between hepatic PEPCK protein, activity, and glyceroneogenesis.

Despite the lack of evidence supporting a decrease in glyceroneogenesis in response to PBDE exposure, other work in the liver suggests that hepatic glyceroneogenesis is responding to changes in hepatic PEPCK activity (Martins-Santos et al., 2007), which has been shown to be suppressed by DE-71 exposure (Nash et al.,

2013). Martins-Santos et al. (2007) incubated precision-cut liver slices from control and 48 h-fasted rats with ^{14}C-glucose, ^{14}C-pyruvate, and ^{14}C-glycerol to measure the contribution of gluconeogenesis, glyceroneogenesis, and glycerol phosphate to the production of glyceride-glycerol in the liver. They found up to a 43% increase in ^{14}C-incorporation from pyruvate in fasted animals compared to controls, supporting an increase in hepatic glyceroneogenesis in the fasted state. Furthermore, Martins-Santos et al. (2007) found an accompanying 84% increase in hepatic PEPCK activity, suggesting glyceroneogenesis responds to changes in hepatic PEPCK activity. This provides evidence to support that the PBDE-induced decrease in hepatic PEPCK activity shown by Nash et al. (2013) may be sufficient to suppress hepatic glyceroneogenesis, which our current data demonstrate.

Furthermore, a recent study conducted by Jaubert et al. (2012) suggested a correlation between PEPCK protein and glyceroneogenesis in the adipose tissue *in vitro*, another finding supported by the current data. Although other work in the adipose tissue contradicts a clear relationship between PEPCK protein, PEPCK activity, and glyceroneogenesis (Nye et al., 2008), it is important to note that this work was done *in vivo*, adding methodological complications that are not seen in *in vitro* models. Additionally, PEPCK activity in the adipose tissue is decreased by glucocorticoids, while PEPCK activity in the liver is increased by glucocorticoids (Chakravarty et al., 2005), suggesting adipose and liver glyceroneogenesis may not be comparable. The current work illustrates that PBDE exposure does indeed decrease hepatic glyceroneogenesis

in addition to hepatic PEPCK protein and activity, supporting a correlation between PEPCK protein, PEPCK activity, and glyceroneogenesis in the liver.

Suppression of glyceroneogenesis seen in the current study in response to DE-71 treatment is expected to cause a lack of glycerol backbone for fatty acid esterification, and a subsequent rise in hepatic non-esterified fatty acids (NEFA). Although we did not measure hepatic NEFA directly, we did measure a significant rise in circulating ketones, suggesting PBDE treatment increased NEFA availability in the liver. It is well established that ketone synthesis is a substrate driven, hepatic pathway dependent on the amount of available NEFA. Once NEFA are delivered to the liver in times of increased lipid mobilization due to fasting, the degree to which ketone synthesis occurs varies, based on the apportioning of those NEFA between oxidation and esterification (Nguyen et al., 2008). Disruptions in the liver's ability to esterify excess NEFA due to suppressed glyceroneogenesis, likely causes a large increase in NEFA oxidation and subsequently, ketogenesis, due to the lack of alternate uses for NEFA within the liver.

Changes in circulating ketones, likely due to suppressed glyceroneogenesis, have been associated with suppression of PEPCK activity, further supporting the relationship between glyceroneogenesis and PEPCK. Ablation of whole body PEPCK in mouse models was sufficient to significantly increase circulating ketones by 3-fold (Hakimi et al., 2005). Silencing of just the mitochondrial form of PEPCK in livers and kidneys of rats was also sufficient to increase circulating ketones by 18% (Stark et al., 2014). No change was exhibited in these or the current study in circulating NFEA levels,

although this is not unexpected. Both CON and TRT animals in the current study were fasted for 48 hours before euthanasia, and changes in circulating NEFA levels between the fed and 48 hour fasted state do not drastically change (Syamsurnarno et al., 2013), despite marked increases in overall energy and lipid metabolism (Sokolovic et al., 2008). This suggests NEFA are transient and circulating levels may not reflect liver-specific changes in metabolism.

Another key finding that exemplifies metabolic disruption by suppressed PEPCK and glyceroneogenesis is the PBDE-induced decrease in circulating triglycerides. This, coupled with the finding that PBDE treatment reduced liver lipids, suggests that PBDE decreased the liver's ability to synthesize triglycerides by suppressing hepatic PEPCK and glyceroneogenesis. This is supported by results from Stark and colleagues (2014), who found that silencing of mitochondrial PEPCK in the liver and kidneys resulted in a 43% decrease in circulating triglycerides. These findings are in contrast to those of Hakimi et al. (2005) who found a 50% increase in circulating triglycerides in response to whole body PEPCK ablation. The key difference in these findings is that one model used whole body PEPCK ablation, while the other monitored tissue specific losses in PEPCK. In adipose tissue, PEPCK plays a key role in triglyceride esterification and storage via glyceroneogenesis. This tissue lacks glycerol kinase as an additional source of glycerol-phosphate, and therefore, if whole body PEPCK is lost, adipose tissue has lost the ability to esterify and store triglycerides, causing an increase in circulating triglyceride levels. The liver, however, has sufficient glycerol kinase, and is therefore still

able to make triglycerides in the absence of PEPCK, adding to the increased levels found in circulation.

The current finding of decreased liver lipid is in contrast to Nash et al. (2013) who demonstrated a significant increase in liver lipid percentage after the same treatment dose and duration of DE-71. One striking difference between the current study and that conducted by Nash et al. (2013) is the state of fasting of the rats. In the current study, rats were fasted for 48 hours to sufficiently stress PEPCK and glyceroneogenesis, whereas in the Nash et al. (2013) study, rats were fasted for only 16 hours. This 32-hour difference in fasting time is significant and could explain key differences in findings in liver lipid, as well as other metabolites such as serum glucose. Indeed, studies in mice have indicated that serum glucose, lactate, and ammonia levels change significantly between a 12-hour and a 48-hour fast, in addition to drastic increases in overall carbohydrate and lipid metabolism (Sokolovic et al., 2008).

Histological data from the current study demonstrates lipid vacuolation in 7 of the 8 Penta-BDE treated rats, and none of the Controls. Although seemingly contradictory to the decreased liver lipids, it was noted that vacuolation was only present midzonally. PEPCK is mainly expressed in the periportal (Gebhardt, 1992) and pericentral regions of the liver lobule (Sato et al., 2014). Because lipid vacuolation in response to PBDE treatment is not occurring in an area of the liver lobule where PEPCK is highly expressed, it may be that fat is reapportioned to the midzonal region, although the reason for this is unclear. Despite midzonal lipid vacuolation seen in treated rats, it is still feasible that total liver lipid is decreased.

As discussed, the current data support that depressed hepatic glyceroneogenesis and its associated consequences occur in response to suppression of hepatic PEPCK activity. This is further accompanied by a decrease in hepatic PEPCK protein. The mechanism by which PBDEs reduce PEPCK protein levels, the likely cause of suppressed PEPCK activity, is unknown. It is well documented that PEPCK is transcriptionally regulated in response to insulin, glucagon, and glucocorticoids through a host of transcription factors (Chakravarty et al., 2005). Preliminary transcriptome profiling of livers from treated rats however, indicates no change in PEPCK message in response to PBDE treatment compared to control (unpublished data). Although these data need to be verified using PEPCK-specific methodology, they suggest our finding of PBDE-associated reductions in PEPCK protein levels may be due to post-translational modifications that are induced by PBDEs and target PEPCK protein for degradation, instead of decreased PEPCK gene transcription. This possibility is supported by demonstrations of three potential mechanisms of post-translational modification of PEPCK, including (1) acetylation (Jiang et al., 2011), (2) ADP-ribosylation (Diani-Moore et al., 2013), and (3) nitration (Jaubert et al., 2012). All three mechanisms target PEPCK for degradation, reducing protein levels. Furthermore, Diani-Moore and colleagues (2013) demonstrated that PEPCK ADP-ribosylation can be a consequence of 2,3,7,8-Tetrachlorodibenzodioxin (TCDD) exposure, so there is precedent for an environmental chemical to initiate post-translational modification of PEPCK protein. Nitration is linked to oxidative stress, a known consequence of PBDE exposure (Jaubert et al., 2012, Albina et al., 2010), and is another possible mechanism of PBDE-

associated decreased PEPCK protein. The role of these mechanisms in PBDE-induced suppression of PEPCK protein have not yet been investigated.

In summary, the findings of this study demonstrate that chronic PBDE-exposure disrupts hepatic lipid metabolism by decreasing glyceroneogenesis, increasing circulating ketones, and decreasing hepatic and circulating triglycerides. In addition, this suppression of hepatic glyceroneogenesis is associated with suppressed hepatic PEPCK protein and activity. However, the effect of environmentally relevant doses of PBDE on hepatic PEPCK and its associated metabolic pathways is still unknown. Whether or not a decrease in hepatic glyceroneogenesis has health-associated relevance, including disruption of insulin signaling via increased NEFA, remains to be determined.

TABLES AND FIGURES

	Final Body Weight (gms)	Liver Weight (gms)	Liver Weight (% Body Weight)
CON	268±5[1]	10.5±0.3[1]	3.9±0.1[1]
TRT	283±6[2]	13.9±0.3[1]*	4.9±0.1[2]*

Table 2. Body and Liver Weight
Final body weight, liver weight and liver as percent body weight for CON and TRT rats. Two-way ANOVA indicated no effect of experiment time, thus the data has been collapsed. There was, however a significant effect of DE-71 treatment. Data are presented as mean ± SEM. [1]n=14, [2]n=13, *p<0.05 compared to CON.

	BDE 47 (ng/g lipid)	BDE 99 (ng/g lipid)	BDE 100 (ng/g lipid)
CON	140.9±43.1	121.9±36.2	25.8±8.0
TRT	8349±888*	3750±487*	2069±217*

Table 3. Liver Burden of relevant PBDE congeners
Final concentrations of the 3 most abundant congeners (accounting for 97-99% of hepatic PBDE burden) present in livers of CON and TRT rats (n=6, mean ± SEM). *p<0.05 compared to CON.

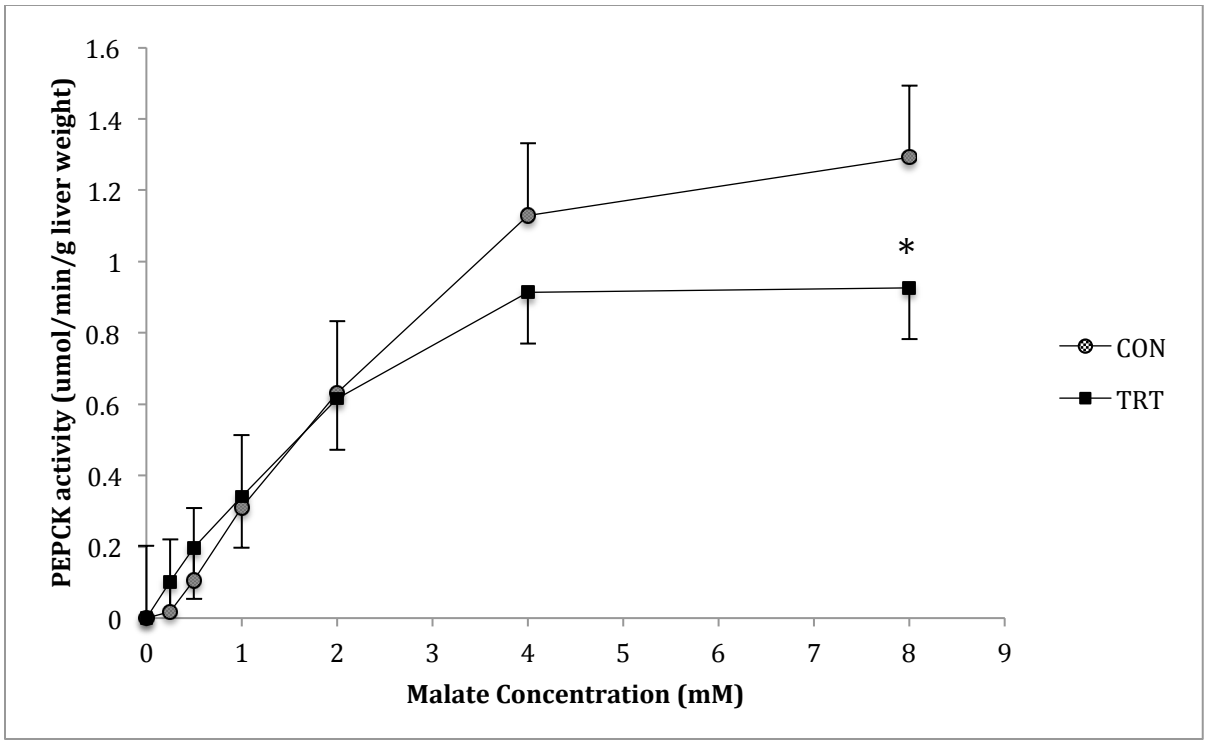

Figure 3. Hepatic PEPCK Activity
Kinetics curve for PEPCK activity in liver from CON (gray circles) and TRT rats (solid black squares) (n=6, mean ± SEM). *p<0.05 compared to CON.

	Vmax (umol/min/g liver)	**Km [malate]**
CON	2.27±0.18[1]	3.05±0.57[2]
TRT	1.36±0.17*[2]	2.85±0.57[2]

Table 4. Hepatic PEPCK enzyme kinetics
PEPCK Vmax and Km in liver from CON and TRT rats. ([1]n=5, [2]n=6, mean ± SEM). *p<0.05 compared to CON.

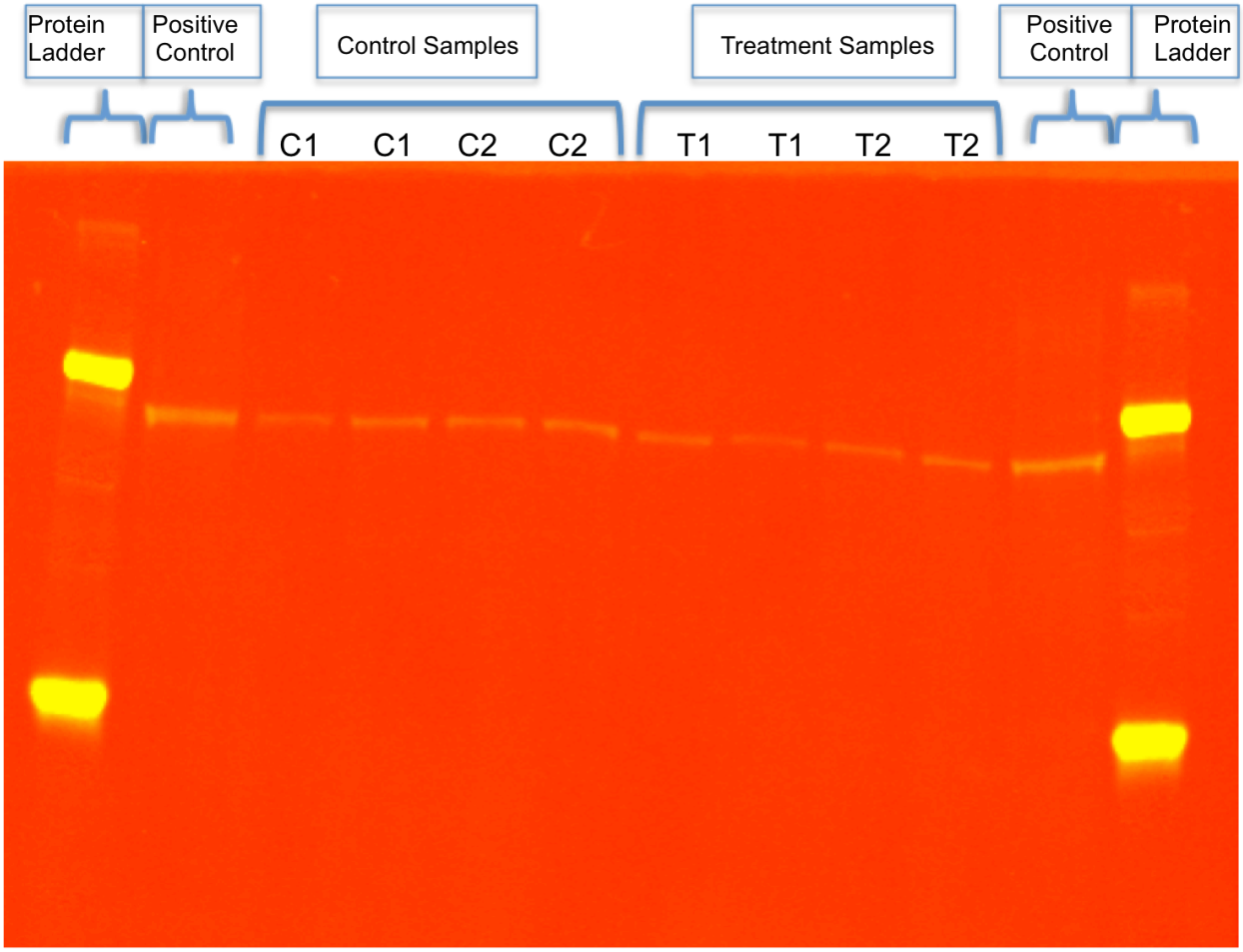

Figure 4. Hepatic PEPCK Protein
Liver protein extracts from CON and TRT rats were separated by 10% SDS-PAGE and PEPCK protein was analyzed by Western blotting. Rat liver extract (Santa Cruz Biotechnology, Dallas, TX) was used as a positive control for hepatic PEPCK. A representative blot comparing duplicate CON and TRT livers is presented (n=2 group).

	Glucose (mg/dL)	Beta-hydroxybutarate (mg/dL)	Triglycerides (mg/dL)	NEFAs (mEq/L)	Cholesterol (mg/dL)
CON	177±19	21.8±1.4	83±1	0.682±0.052	78±6
TRT	92±5*	27.7±1.5*	61±7*	0.635±0.037	69±6

Table 5. Blood Metabolites
Serum metabolites for CON and TRT rats following 28 days treatment and subsequent 48-hour fast (n=8, mean ± SEM). *p<0.05 compared to CON.

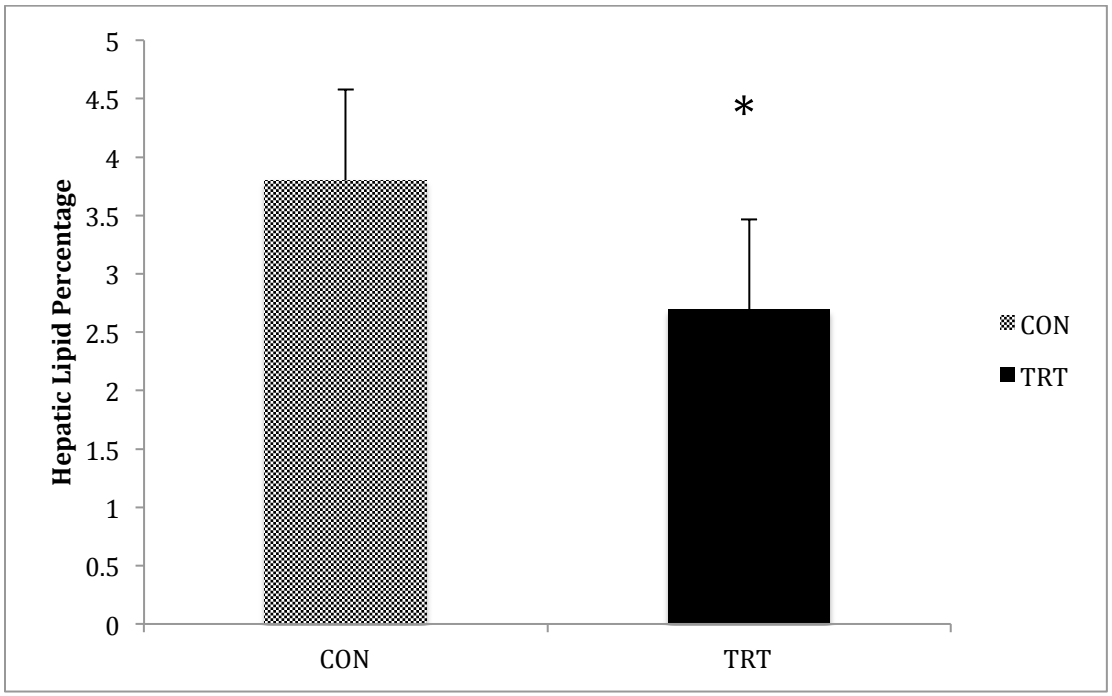

Figure 5. Hepatic Lipid Percentage
Lipid extracted from livers is presented as a percentage of total liver weight for both CON (gray) and TRT (solid black) rats (n=6, mean ± SEM). *p<0.05 compared to CON.

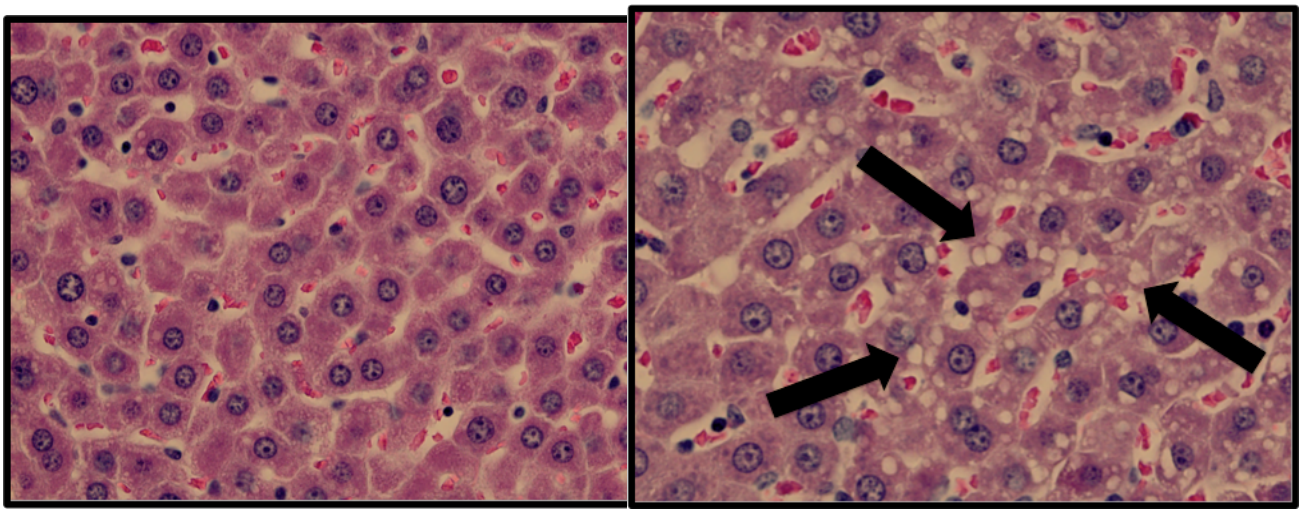

4A - Control 4B - Penta-BDE

Figure 6. Histological Examination of Hepatic Lipid Content
Representative photos of liver sections from CON and TRT rats evaluated by light microscopy at 40x magnification. (4A) CON exhibited normal hepatic cellular appearance. (4B) TRT had visible fatty vacuolation throughout the mid-zonal region that was not found in liver tissue from CON rats. Black arrows indicate fat vacuoles.

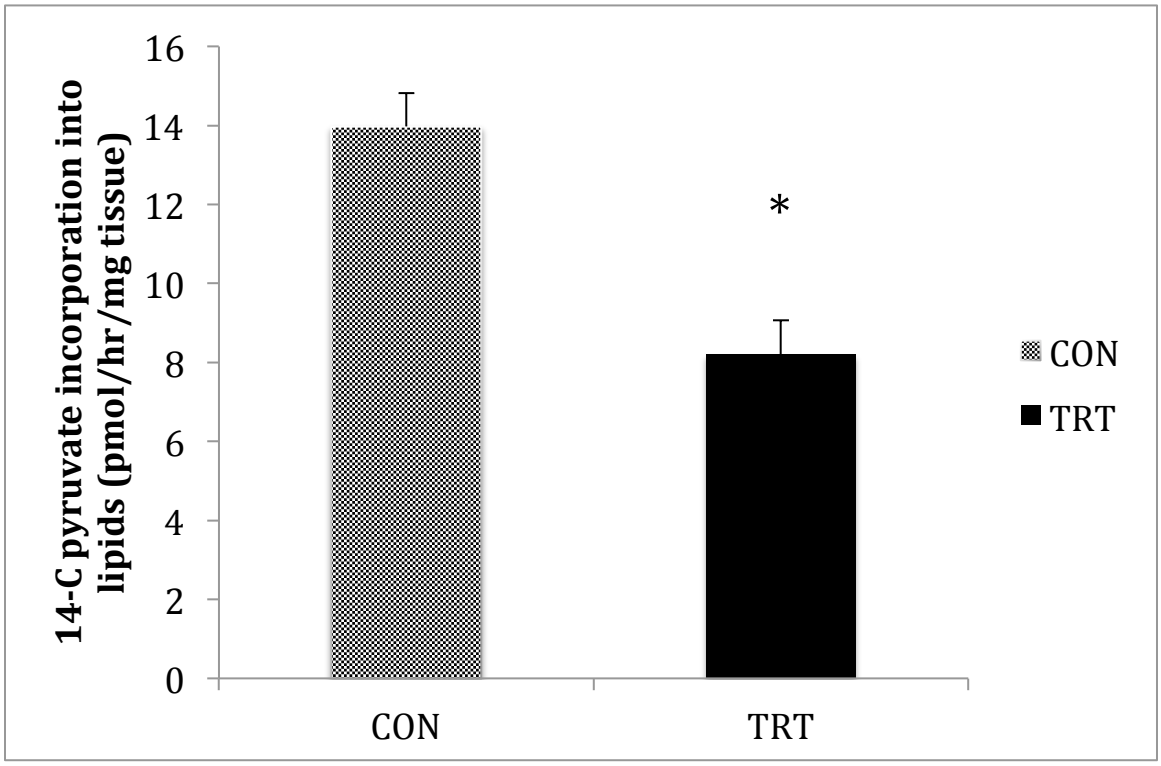

Figure 7. *In Vitro* Hepatic Glyceroneogenesis
Rates of glyceroneogenesis in liver explants from CON (gray) and TRT (solid) rats (n=6, mean ± SEM). *$p<0.05$ compared to CON.

APPENDICES

APPENDIX A

Transcriptome Data

Gene	Protein	Fold change (TRT vs. CON livers)
Cyp2b1	Cytochrome P450, family 2, subfamily B, polypeptide 1	1.80E+308
Cyp1a1	Cytochrome P450, family 1, subfamily A, polypeptide 1	553.26
LOC100909962	Cytochrome P450 2B1-like	74.47
Cyp2b2	Cytochrome P450, family 2, subfamily B, polypeptide 1	44.86
Cyp2c6v1 (NW_003806290 1395..6073)	Cytochrome P450, family 2, subfamily C, polypeptide 6, variant 1	7.25
Fabp4	Fatty acid binding protein 4	6.86
Ugt2b1	UDP glucuronosyltransferase 2 family, polypeptide B1	6.73
Rnf13 (NW_003807001 776757..811777)	Ring finger protein 13	6.43
LOC100910385	Peroxisomal acyl-coenzyme A oxidase 1-like	5.92
Ugt2b	UDP glycosyltransferase 2 family, polypeptide B	5.43
Dhtkd1 (NW_003812525 173027..232220)	Dehydrogenase E1 and transketolase domain containing 1	4.80
Dhcr24	24-dehydrocholesterol reductase	4.75
C5 (NW_003807440 1439..23515)	Complement component 5	4.70
Rxra	Retinoid x receptor alpha	4.57
LOC100364457	Ribosomal protein L9-like	4.47
Rn18s	18s ribosomal RNA	3.91
Adipor2	Adiponectin receptor 2	3.75
Abhd2	Abhydrolase domain containing 2	3.71
Aldh1a1	Aldehyde dehydrogenase 1 family, member A1	3.37
LOC257642	rRNA promoter binding protein	3.23
Cpamd8 (NW_003808236 6132..8613)	C3 and PZP-like, alpha-2-macroglobulin domain containing 8	3.18

Cyp2c6v1 (NW_003806294 23625..120993)	Cytochrome P450, family 2, subfamily C, polypeptide 6, variant 1	3.14
Hnf4a	Hepatocyte nuclear factor 4, alpha	2.88
Abcb11 (NW_003807561 2064..90772)	ATP-binding cassette, subfamily B (MDR/TAP), member 11	2.87
Mpeg1	Macrophage expressed 1	2.85
Afm (NW_003811475 589..4764)	Afamin	2.84
Cyp1a2	Cytochrome P450, family 1, subfamily A, polypeptide 2	2.78
Ces2a (NW_003812795 59045..64825)	Carboxylesterase 2A	2.77
Abcc2	ATP-binding cassette, subfamily C (CFTR/MRP), member 2	2.67
Lonp2	Ion peptidase 2, peroxisomal	2.61
Mup4	Major urinalry protein 4	2.55
Ephx1	Epoxide hydrolase 1, microsomal (xenobiotic)	2.38
LOC100362027	Ribosomal protein L30-like	2.35
Acox1	Acyl-CoA oxidase 1, palmitoyl	2.33
Cyp3a85-ps	Cytochrome P450, family 3, subfamily A, polypeptide 85, pseudogene	2.19
LOC100909666	Complement C4-like	2.19
LOC100911718	Cytochrome p450 2C6-like	2.14
Slco1b3	Solute carrier organic anion transporter family, member 1B3	2.07
LOC100359498	Ribosomal protein L35a-like	-2.01
Hba-a2	Hemoglobin alpha, adult chain 2	-2.07
Hbb	Hemoglobin, beta	-2.08
LOC360504	Hemoglobin, alpha 2	-2.27
LOC100134871	Beta globin minor gene	-2.43
Rpl30	Ribosomal protein L30	-2.45
Hbb-b1	Hemoglobin, beta adult major chain	-2.47
Rps26	Ribosomal protein S26	-2.51
LOC689064	Beta-globin	-2.72
LOC100912411	Uncharacterized	-2.79
Rpl9	Ribosomal protein L9	-2.81

To assess changes in gene expression of PEPCK, a library of mRNA expression was created. Sixteen, male weanling Wistar rats were treated daily with 14 mg/kg body weight DE-71 (TRT, n=8) or corn oil vehicle (CON, n=8) for 28 days. Rats were euthanized after a 16 hr fast and livers were frozen. To reduce biological variability, 100 mg frozen tissue was dissected from 10 randomly selected livers from the CON (n=5) and TRT (n=5) groups. The samples were then pooled within groups, resulting in 1-500mg representative CON sample and 1-500mg representative TRT sample. Tissue

could not be thawed at any time during the pooling process, so dissection of frozen tissue was done quickly using a scalpel and tweezers in a walk-in refrigerator.

RNA was extracted from the CON and TRT samples using a commercially available RiboPure kit (Ambion, Life Technologies). RNA samples were then sent to the Hubbard Center for Genomic study at the University of New Hampshire for subsequent mRNA extraction and gene sequencing. A library of genes expressed in the liver was made using cDNA for both CON and TRT. Relative expression was quantified using an Illumina HiSeq 2500 sequencer, and mapped to the reference genome of the Wistar rat. Data are expressed as fold change in gene expression in TRT livers compared to CON. There was no change in hepatic PEPCK-c or PEPCK-m in TRT livers compared to CON. Genes that changed by 2-fold or greater in response to DE-71 are presented.

APPENDIX B

Glyceroneogenesis Between-Animal Coefficient of Variation

Animal ID	Glyceroneogenesis Rate (pmol/hr/mg tissue)	Average between animals	Standard Deviation	Coefficient of Variation
P1	13.57	14.61	1.27	8.67%
P2	14.96			
P3	13.39			
P4	16.54			

To determine biological variation between animals for the glyceroneogenesis assay and inform animal numbers necessary for subsequent experiments, four adult rats were sacrificed and livers removed. Three-200 mg portions were taken from each liver and used for glyceroneogenesis quantification. Each sample was run in duplicate. Duplicates were averaged within each sample, and triplicates were then averaged within each animal. The average and standard deviation between animals was used to calculate the between-animal coefficient of variation.

APPENDIX C

Glyceroneogenesis Within-Animal Coefficient of Variation

Sample ID	Glyceroneogenesis rate (pmol/hr/mg tissue)	Average within animals	Standard Deviation	Coefficient of Variation
P5-1	15.04	14.85	1.64	11.09%
P5-2	14.34			
P5-3	15.39			
P5-4	17.91			
P5-5	13.12			
P5-6	15.32			
P5-7	14.71			
P5-8	16.10			
P5-9	11.74			

To determine biological variability within the liver for the glyceroneogenesis assay, one adult rat was sacrificed and the liver was removed. Nine-200 mg portions were taken from the liver and used for glyceroneogenesis quantification. Each sample was run in duplicate. Duplicates were averaged within each sample, and then all nine samples were averaged. The average and standard deviation was used to calculate the within-animal coefficient of variation.

APPENDIX D

PEPCK Activity in Subcutaneous Adipose Tissue

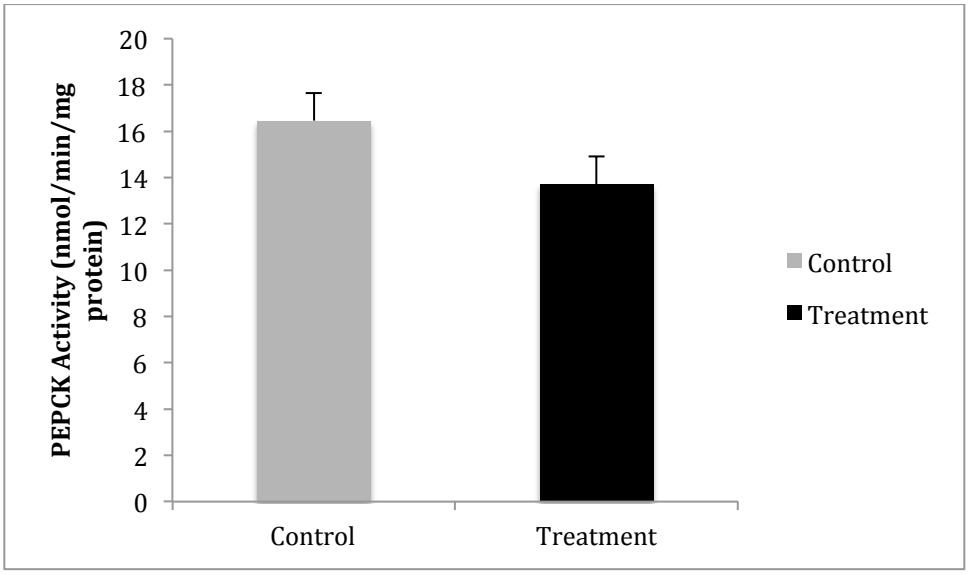

To assess changes in PEPCK activity in adipose tissue, 16 male, weanling Wistar rats were treated daily with 14 mg/kg bw DE-71 (TRT, n=8) or corn oil vehicle (CON, n=8) for 28 days. After a 16 hr fast, rats were euthanized and epididymal fat pads removed, weighed, and placed in 10% saline solution for transport to the lab. Fat tissue was homogenized and centrifuged at 23426 x g for cytosol isolation. PEPCK activity was quantified as previously described (Nye et al., 2008). PEPCK activity in TRT adipose tissue was suppressed by 17% compared to CON (p=0.068).

APPENDIX E

Serum Metabolites

METABOLITE	CON	TRT
Glucose (mg/dL)	177 ± 19	95 ± 5*
Beta-hydroxybutarate (mg/dL)	21.8 ± 1.4	27.7 ± 1.5*
Triglycerides (mg/dL)	83 ± 1	61 ± 7*
NEFA (mEq/L)	0.682 ± 0.052	0.635 ± 0.037
Cholesterol (mg/dL)	78 ± 6	69 ± 6
Alanine Transaminase (U/L)	24 ± 1	27 ± 2
Alkaline Phosphatase (U/L)	165 ± 11	145 ± 9
Total Bilirubin (mg/dL)	.01 ± .04	.01 ± .04
Total Protein (g/dL)	6.6 ± .1	6.5 ± 0.1
Albumin (g/dL)	3.6 ± 0.1	3.6 ± 0.1
Urea Nitrogen (mg/dL)	15 ± 1	13 ± 1
Creatinine (mg/dL)	0.3 ± 0.01	0.3 ± 0.02
Calcium (mg/dL)	12.6 ± 0.1	12.2 ± 0.2
Sodium (mmol/L)	147 ± 1	149 ± 0.5
Potassium (mmol/L)	7.9 ± 0.3	7.6 ± 0.2
Chloride (mmol/L)	98 ± 1	100 ± 1
Globulin (g/dL)	3.0 ± 0.05	2.9 ± 0.03
Albumin/Globulin Ratio	1.2 ± .03	1.2 ± 0.03
Urea/Creatinine Ratio	52 ± 2	50 ± 4
Sodium/Potassium Ratio	19 ± 1	20 ± 1

To assess metabolic changes associated with PBDE exposure, 16 male, weanling Wistar rats were treated daily with 14 mg/kg bw DE-71 (TRT, n=8) or corn oil vehicle (CON, n=8) for 28 days. Rats were euthanized after a 48 hr fast and blood was collected via cardiac puncture. Serum was separated and sent to Marshfield Laboratories (Marshfield, WI) for metabolite quantification. A complete metabolic serum profile of CON and TRT animals is presented; selected metabolites are listed in Table 5. Data are presented as mean ± SE, *$p<0.05$.

APPENDIX F

Hepatic PBDE Congeners

PBDE Congener	CON (ng/g lipid)	TRT (ng/g lipid)
BDE 100	25.8 ± 8.0	2069 ± 217*
BDE 99	121.9 ± 36.2	3750 ± 487*
BDE 47	140.9 ± 43.1	8349 ± 888*
BDE 28, 33	1.1 ± 0.3	21.5 ± 2.8*
BDE 49	1.3 ± 0.4	2.7 ± 0.4*
BDE 66	1.4 ± 0.7	5.7 ± 0.3*
BDE 85, 155	5.4 ± 1.9	503.5 ± 49.8*
Total	297.5 ± 88.6	14701 ± 1603*

To determine hepatic PBDE burden in response to chronic high DE-71 treatment, 12 male, weanling Wistar rats were treated daily with 14 mg/kg bw DE-71 (TRT, n=6) or corn oil vehicle (CON, n=6) for 28 days. After a 48 hr fast, rats were euthanized, and livers were removed and frozen in 2 gram portions. Frozen livers were sent to Dr. Heather Stapleton at Duke University for analysis of PBDE congeners. A complete profile of BDE congeners measured in CON and TRT livers is presented. Data are presented as mean±SE, *$p<0.05$.

APPENDIX G

IACUC Approval Letter – Experiment 1

University *of* New Hampshire

Research Integrity Services, Service Building
51 College Road, Durham, NH 03824-3585
Fax: 603-862-3564

25-Oct-2013

Carey, Gale B
Molecular, Cellular & Biomedical Sciences, Kendall Hall
Durham, NH 03824

IACUC #: 131003
Project: Polybrominated Diphenyl Ethers and Diabetes
Category: E
Approval Date: 17-Oct-2013

The Institutional Animal Care and Use Committee (IACUC) reviewed and approved the protocol submitted for this study under Category E on Page 5 of the Application for Review of Vertebrate Animal Use in Research or Instruction - *Animal use activities that involve accompanying pain or distress to the animals for which appropriate anesthetic, analgesic, tranquilizing drugs or other methods for relieving pain or distress are not used.*

Approval is granted for a period of three years from the approval date above. Continued approval throughout the three year period is contingent upon completion of annual reports on the use of animals. At the end of the three year approval period you may submit a new application and request for extension to continue this project. Requests for extension must be filed prior to the expiration of the original approval.

Please Note:
1. All cage, pen, or other animal identification records must include your IACUC # listed above.
2. Use of animals in research and instruction is approved contingent upon participation in the UNH Occupational Health Program for persons handling animals. Participation is mandatory for all principal investigators and their affiliated personnel, employees of the University and students alike. Information about the program, including forms, is available at http://unh.edu/research/occupational-health-program-animal-handlers.

If you have any questions, please contact either Dean Elder at 862-4629 or Julie Simpson at 862-2003.

For the IACUC,

Jill A. McGaughy, Ph.D.
Chair

cc: File

APPENDIX H

IACUC Approval Letter – Experiment 2

University *of* New Hampshire

Research Integrity Services, Service Building
51 College Road, Durham, NH 03824-3585
Fax: 603-862-3564

01-Aug-2014

Carey, Gale B
Molecular, Cellular & Biomedical Sciences, Kendall Hall
Durham, NH 03824

IACUC #: 140701
Project: Persistent Organic Pollutants and Hepatic PEPCK Activity
Category: E
Approval Date: 17-Jul-2014

The Institutional Animal Care and Use Committee (IACUC) reviewed and approved the protocol submitted for this study under Category E on Page 5 of the Application for Review of Vertebrate Animal Use in Research or Instruction - *Animal use activities that involve accompanying pain or distress to the animals for which appropriate anesthetic, analgesic, tranquilizing drugs or other methods for relieving pain or distress are not used.*

Approval is granted for a period of three years from the approval date above. Continued approval throughout the three year period is contingent upon completion of annual reports on the use of animals. At the end of the three year approval period you may submit a new application and request for extension to continue this project. Requests for extension must be filed prior to the expiration of the original approval.

Please Note:
1. All cage, pen, or other animal identification records must include your IACUC # listed above.
2. Use of animals in research and instruction is approved contingent upon participation in the UNH Occupational Health Program for persons handling animals. Participation is mandatory for all principal investigators and their affiliated personnel, employees of the University and students alike. Information about the program, including forms, is available at http://unh.edu/research/occupational-health-program-animal-handlers.

If you have any questions, please contact me at 862-4629 or Julie Simpson at 862-2003.

For the IACUC,

Dean Elder, D.V.M.
Vice Chair

cc: File

References

1. Albina ML, Alonso V, Linares V, Belles M, Sirvent JJ, Domingo JL, Sanchez DJ. Effects of exposure to BDE-99 on oxidative status of liver and kidney in adult rats. Toxicology 2010 Apr 30;271(1-2):51-6.

2. An J, Li S, Zhong Y, Wang Y, Zhen K, Zhang X, Wang Y, Wu M, Yu Z, Sheng G, et al. The cytotoxic effects of synthetic 6-hydroxylated and 6-methoxylated polybrominated diphenyl ether 47 (BDE47). Environ Toxicol 2011 Nov;26(6):591-9.

3. Athanasiadou M, Cuadra SN, Marsh G, Bergman A, Jakobsson K. Polybrominated diphenyl ethers (PBDEs) and bioaccumulative hydroxylated PBDE metabolites in young humans from managua, nicaragua. Environ Health Perspect 2008 Mar;116(3):400-8.

4. Berndtson WE. A simple, rapid and reliable method for selecting or assessing the number of replicates for animal experiments. J Anim Sci 1991 Jan;69(1):67-76.

5. Besis A, Samara C. Polybrominated diphenyl ethers (PBDEs) in the indoor and outdoor environments--a review on occurrence and human exposure. Environ Pollut 2012 Oct;169:217-29.

6. Boden G. Fatty acid-induced inflammation and insulin resistance in skeletal muscle and liver. Curr Diab Rep 2006 Jun;6(3):177-81.

7. Boden G. Role of fatty acids in the pathogenesis of insulin resistance and NIDDM. Diabetes 1997 Jan;46(1):3-10.

8. Boden G, Chen X, Ruiz J, White JV, Rossetti L. Mechanisms of fatty acid-induced inhibition of glucose uptake. J Clin Invest 1994 Jun;93(6):2438-46.

9. Boden G, Jadali F. Effects of lipid on basal carbohydrate metabolism in normal men. Diabetes 1991 Jun;40(6):686-92.

10. Bruchajzer E, Frydrych B, Sporny S, Szymanska JA. Toxicity of penta- and decabromodiphenyl ethers after repeated administration to rats: A comparative study. Arch Toxicol 2010 Apr;84(4):287-99.

11. Canton RF, Sanderson JT, Letcher RJ, Bergman A, van den Berg M. Inhibition and induction of aromatase (CYP19) activity by brominated flame retardants in H295R human adrenocortical carcinoma cells. Toxicol Sci 2005 Dec;88(2):447-55.

12. Capurso C, Capurso A. From excess adiposity to insulin resistance: The role of free fatty acids. Vascul Pharmacol 2012 Sep-Oct;57(2-4):91-7.

13. Chakravarty K, Cassuto H, Reshef L, Hanson RW. Factors that control the tissue-specific transcription of the gene for phosphoenolpyruvate carboxykinase-C. Crit Rev Biochem Mol Biol 2005 May-Jun;40(3):129-54.

14. Costa LG, Giordano G. Developmental neurotoxicity of polybrominated diphenyl ether (PBDE) flame retardants. Neurotoxicology 2007 Nov;28(6):1047-67.

15. Costa LG, Giordano G, Tagliaferri S, Caglieri A, Mutti A. Polybrominated diphenyl ether (PBDE) flame retardants: Environmental contamination, human body burden and potential adverse health effects. Acta Biomed 2008 Dec;79(3):172-83.

16. Covaci A, Voorspoels S, Roosens L, Jacobs W, Blust R, Neels H. Polybrominated diphenyl ethers (PBDEs) and polychlorinated biphenyls (PCBs) in human liver and adipose tissue samples from Belgium. Chemosphere 2008 Sep;73(2):170-5.

17. Dedkova EN, Blatter LA. Role of beta-hydroxybutyrate, its polymer poly-beta-hydroxybutyrate and inorganic polyphosphate in mammalian health and disease. Front Physiol 2014 Jul 17;5:260.

18. Diani-Moore S, Zhang S, Ram P, Rifkind AB. Aryl hydrocarbon receptor activation by dioxin targets phosphoenolpyruvate carboxykinase (PEPCK) for ADP-ribosylation via 2,3,7,8-tetrachlorodibenzo-p-dioxin (TCDD)-inducible poly(ADP-ribose) polymerase (TiPARP). J Biol Chem 2013 Jul 26;288(30):21514-25.

19. Dunn RL, Huwe JK, Carey GB. Biomonitoring polybrominated diphenyl ethers in human milk as a function of environment, dietary intake, and demographics in New Hampshire. Chemosphere 2010 Aug;80(10):1175-82.

20. Feo ML, Gross MS, McGarrigle BP, Eljarrat E, Barcelo D, Aga DS, Olson JR. Biotransformation of BDE-47 to potentially toxic metabolites is predominantly mediated by human CYP2B6. Environ Health Perspect 2013 Apr;121(4):440,6, 446e1-7.

21. Frederiksen M, Vorkamp K, Thomsen M, Knudsen LE. Human internal and external exposure to PBDEs--a review of levels and sources. Int J Hyg Environ Health 2009 Mar;212(2):109-34.

22. Gebhardt R. Metabolic zonation of the liver: Regulation and implications for liver function. Pharmacol Ther 1992;53(3):275-354.

23. Griffin ME, Marcucci MJ, Cline GW, Bell K, Barucci N, Lee D, Goodyear LJ, Kraegen EW, White MF, Shulman GI. Free fatty acid-induced insulin resistance is associated with activation of protein kinase C theta and alterations in the insulin signaling cascade. Diabetes 1999 Jun;48(6):1270-4.

24. Hakimi P, Johnson MT, Yang J, Lepage DF, Conlon RA, Kalhan SC, Reshef L, Tilghman SM, Hanson RW. Phosphoenolpyruvate carboxykinase and the critical role of cataplerosis in the control of hepatic metabolism. Nutr Metab (Lond) 2005 Nov 21;2:33.

25. Hale RC, Kim SL, Harvey E, La Guardia MJ, Mainor TM, Bush EO, Jacobs EM. Antarctic research bases: Local sources of polybrominated diphenyl ether (PBDE) flame retardants. Environ Sci Technol 2008 Mar 1;42(5):1452-7.

26. Hamers T, Kamstra JH, Sonneveld E, Murk AJ, Kester MH, Andersson PL, Legler J, Brouwer A. In vitro profiling of the endocrine-disrupting potency of brominated flame retardants. Toxicol Sci 2006 Jul;92(1):157-73.

27. Hanson RW, Patel YM. Phosphoenolpyruvate carboxykinase (GTP): The gene and the enzyme. Adv Enzymol Relat Areas Mol Biol 1994;69:203-81.

28. Harrad S, Ibarra C, Diamond M, Melymuk L, Robson M, Douwes J, Roosens L, Dirtu AC, Covaci A. Polybrominated diphenyl ethers in domestic indoor dust from Canada, New Zealand, United Kingdom and United States. Environ Int 2008 Feb;34(2):232-8.

29. Jaubert AM, Penot G, Niang F, Durant S, Forest C. Rapid nitration of adipocyte phosphoenolpyruvate carboxykinase by leptin reduces glyceroneogenesis and induces fatty acid release. PLoS One 2012;7(7):e40650.

30. Jiang W, Wang S, Xiao M, Lin Y, Zhou L, Lei Q, Xiong Y, Guan KL, Zhao S. Acetylation regulates gluconeogenesis by promoting PEPCK1 degradation via recruiting the UBR5 ubiquitin ligase. Mol Cell 2011 Jul 8;43(1):33-44.

31. Johnson-Restrepo B, Kannan K, Rapaport DP, Rodan BD. Polybrominated diphenyl ethers and polychlorinated biphenyls in human adipose tissue from New York. Environ Sci Technol 2005 Jul 15;39(14):5177-82.

32. Jones-Otazo HA, Clarke JP, Diamond ML, Archbold JA, Ferguson G, Harner T, Richardson GM, Ryan JJ, Wilford B. Is house dust the missing exposure pathway for PBDEs? an analysis of the urban fate and human exposure to PBDEs. Environ Sci Technol 2005 Jul 15;39(14):5121-30.

33. Kalhan SC, Bugianesi E, McCullough AJ, Hanson RW, Kelley DE. Estimates of hepatic glyceroneogenesis in type 2 diabetes mellitus in humans. Metabolism 2008 Mar;57(3):305-12.

34. Kalhan SC, Mahajan S, Burkett E, Reshef L, Hanson RW. Glyceroneogenesis and the source of glycerol for hepatic triacylglycerol synthesis in humans. J Biol Chem 2001 Apr 20;276(16):12928-31.

35. Kalhan SC, Mahajan S, Burkett E, Reshef L, Hanson RW. Glyceroneogenesis and the source of glycerol for hepatic triacylglycerol synthesis in humans. J Biol Chem 2001 Apr 20;276(16):12928-31.

36. Kanikarla-Marie P, Jain SK. Hyperketonemia (acetoacetate) upregulates NADPH oxidase 4 and elevates oxidative stress, ICAM-1, and monocyte adhesivity in endothelial cells. Cell Physiol Biochem 2015;35(1):364-73.

37. Lee E, Kim TH, Choi JS, Nabanata P, Kim NY, Ahn MY, Jung KK, Kang IH, Kim TS, Kwack SJ, et al. Evaluation of liver and thyroid toxicity in Sprague-Dawley rats after exposure to polybrominated diphenyl ether BDE-209. J Toxicol Sci 2010 Aug;35(4):535-45.

38. Marchesini GR, Meimaridou A, Haasnoot W, Meulenberg E, Albertus F, Mizuguchi M, Takeuchi M, Irth H, Murk AJ. Biosensor discovery of thyroxine transport disrupting chemicals. Toxicol Appl Pharmacol 2008 Oct 1;232(1):150-60.

39. Martins-Santos ME, Chaves VE, Frasson D, Boschini RP, Garofalo MA, Kettelhut Ido C, Migliorini RH. Glyceroneogenesis and the supply of glycerol-3-phosphate for glyceride-glycerol synthesis in liver slices of fasted and diabetic rats. Am J Physiol Endocrinol Metab 2007 Nov;293(5):E1352-7.

40. McDonald TA. A perspective on the potential health risks of PBDEs. Chemosphere 2002 Feb;46(5):745-55.

41. Meerts IA, van Zanden JJ, Luijks EA, van Leeuwen-Bol I, Marsh G, Jakobsson E, Bergman A, Brouwer A. Potent competitive interactions of some brominated flame retardants and related compounds with human transthyretin in vitro. Toxicol Sci 2000 Jul;56(1):95-104.

42. Nash JT, Szabo DT, Carey GB. Polybrominated diphenyl ethers alter hepatic phosphoenolpyruvate carboxykinase enzyme kinetics in male Wistar rats: Implications for lipid and glucose metabolism. J Toxicol Environ Health A 2013;76(2):142-56.

43. Nguyen P, Leray V, Diez M, Serisier S, Le Bloc'h J, Siliart B, Dumon H. Liver lipid metabolism. J Anim Physiol Anim Nutr (Berl) 2008 Jun;92(3):272-83.

44. Nye CK, Hanson RW, Kalhan SC. Glyceroneogenesis is the dominant pathway for triglyceride glycerol synthesis in vivo in the rat. J Biol Chem 2008 Oct 10;283(41):27565-74.

45. Osako M, Kim YJ, Sakai S. Leaching of brominated flame retardants in leachate from landfills in japan. Chemosphere 2004 Dec;57(10):1571-9.

46. Rains JL, Jain SK. Effect of hyperketonemia (acetoacetate) on nuclear factor-kappaB and p38 mitogen-activated protein kinase activation mediated intercellular adhesion molecule 1 upregulation in endothelial cells. Metab Syndr Relat Disord 2015 Mar;13(2):71-7.

47. Ruehl-Fehlert C, Kittel B, Morawietz G, Deslex P, Keenan C, Mahrt CR, Nolte T, Robinson M, Stuart BP, Deschl U, et al. Revised guides for organ sampling and trimming in rats and mice--part 1. Exp Toxicol Pathol 2003 Sep;55(2-3):91-106.

48. Sato A, Kadokura K, Uchida H, Tsukada K. An in vitro hepatic zonation model with a continuous oxygen gradient in a microdevice. Biochem Biophys Res Commun 2014 Oct 31;453(4):767-71.

49. She P, Shiota M, Shelton KD, Chalkley R, Postic C, Magnuson MA. Phosphoenolpyruvate carboxykinase is necessary for the integration of hepatic energy metabolism. Mol Cell Biol 2000 Sep;20(17):6508-17.

50. Sjodin A, Wong LY, Jones RS, Park A, Zhang Y, Hodge C, Dipietro E, McClure C, Turner W, Needham LL, et al. Serum concentrations of polybrominated diphenyl ethers (PBDEs) and polybrominated biphenyl (PBB) in the united states population: 2003-2004. Environ Sci Technol 2008 Feb 15;42(4):1377-84.

51. Sokolovic M, Sokolovic A, Wehkamp D, Ver Loren van Themaat E, de Waart DR, Gilhuijs-Pederson LA, Nikolsky Y, van Kampen AH, Hakvoort TB, Lamers WH. The transcriptomic signature of fasting murine liver. BMC Genomics 2008 Nov 6;9:528.

52. Stapleton HM, Kelly SM, Pei R, Letcher RJ, Gunsch C. Metabolism of polybrominated diphenyl ethers (PBDEs) by human hepatocytes in vitro. Environ Health Perspect 2009 Feb;117(2):197-202.

53. Stark R, Guebre-Egziabher F, Zhao X, Feriod C, Dong J, Alves TC, Ioja S, Pongratz RL, Bhanot S, Roden M, et al. A role for mitochondrial phosphoenolpyruvate carboxykinase (PEPCK-M) in the regulation of hepatic gluconeogenesis. J Biol Chem 2014 Mar 14;289(11):7257-63.

54. Thuresson K, Bergman K, Rothenbacher K, Herrmann T, Sjolin S, Hagmar L, Papke O, Jakobsson K. Polybrominated diphenyl ether exposure to electronics recycling workers--a follow up study. Chemosphere 2006 Sep;64(11):1855-61.

55. Tseng LH, Li MH, Tsai SS, Lee CW, Pan MH, Yao WJ, Hsu PC. Developmental exposure to decabromodiphenyl ether (PBDE 209): Effects on thyroid hormone and hepatic enzyme activity in male mouse offspring. Chemosphere 2008 Jan;70(4):640-7.

56. Watkins DJ, McClean MD, Fraser AJ, Weinberg J, Stapleton HM, Sjodin A, Webster TF. Exposure to PBDEs in the office environment: Evaluating the relationships between dust, handwipes, and serum. Environ Health Perspect 2011 Sep;119(9):1247-52.

57. Watkins DJ, McClean MD, Fraser AJ, Weinberg J, Stapleton HM, Sjodin A, Webster TF. Exposure to PBDEs in the office environment: Evaluating the relationships between dust, handwipes, and serum. Environ Health Perspect 2011 Sep;119(9):1247-52.

58. Wilford BH, Shoeib M, Harner T, Zhu J, Jones KC. Polybrominated diphenyl ethers in indoor dust in Ottawa, Canada: Implications for sources and exposure. Environ Sci Technol 2005 Sep 15;39(18):7027-35.

59. Wu N, Herrmann T, Paepke O, Tickner J, Hale R, Harvey LE, La Guardia M, McClean MD, Webster TF. Human exposure to PBDEs: Associations of PBDE body burdens with food consumption and house dust concentrations. Environ Sci Technol 2007 Mar 1;41(5):1584-9.

60. Yang J, Kalhan SC, Hanson RW. What is the metabolic role of phosphoenolpyruvate carboxykinase? J Biol Chem 2009 Oct 2;284(40):27025-9.

61. Zhang W, Sargis RM, Volden PA, Carmean CM, Sun XJ, Brady MJ. PCB 126 and other dioxin-like PCBs specifically suppress hepatic PEPCK expression via the aryl hydrocarbon receptor. PLoS One 2012;7(5):e37103.